university of groningen

faculty of science and engineering

Chaotic dynamics in a periodically forced fold-and-twist map

Master's Project Mathematics

September 2022

Student: R. K. IJpma

First supervisor: dr. A. E. Sterk

Second supervisor: dr. H. Jardón Kojakhmetov

Abstract

Non-invertible planar maps with folds have proven to be a generous source of folded chaotic attractors, although rigorous proofs for their Hénon-like structure are still sought after. The folding maps provide interesting obstacles when embarking upon constructing such proofs, but they also provide a new source for so-called *quasi-periodic Hénon-like* attractors. Such attractors coincide with the closure of the unstable manifold of a quasi-periodic invariant circle, on which the dynamics are loosely speaking 'Hénon-like product quasi-periodic'. We provide numerical evidence for such attractors in a periodically driven fold-and-twist map, occurring for sets of parameters with positive measure. We also find that discovering promising proof strategies for the existence of these attractors remains troublesome, due to the non-dissipativity of the fold-and-twist map, and unwieldy changes in periodicity of saddle points when perturbing parameters.

Contents

1. Introduction

Within the field of non-linear dynamics, there is ample study on the behaviour of invertible maps. This is not surprising, for invertible maps are in many respects easier to manipulate than their non-invertible counterparts. However, since processes in nature are typically irreversible, the non-invertible case becomes important to study eventually. In particular, the chaotic regimes of continuous maps are of interest, and this is an area where non-invertible maps can display phenomena which invertible maps cannot.

Consider for example the irreversible time evolution of a planar point (x, y) given by the recurrence relation

$$\begin{aligned} x_{n+1} &= ax_n(1 - x_n - y_n), \\ y_{n+1} &= bx_n y_n. \end{aligned}$$

The above equations can be viewed as a map $P : (x_n, y_n) \longmapsto (x_{n+1}, y_{n+1})$, depending on two real parameters $a > 1$ and $b > 1$. It is a model for a predator-prey system, where at time n, x_n represents the number of prey, y_n represents the number of predators, and one unit of time spans the life of each predator. The map P has two key properties which determine its global behaviour. Firstly, if $b > (a+\sqrt{a})/(2a-2)$, then the fixed point $(\frac{1}{b}, 1-\frac{1}{a}-\frac{1}{b})$ has complex eigenvalues. Secondly, P maps two-to-one onto the half plane $ab - 4bx - 4ay > 0$. In other words, P rotates points around the fixed point, and it folds the plane in a line away from the fixed point. For certain parameter values, iterating this action leads to seemingly chaotic behaviour, as shown in Figure 1. In particular, the iterates appear to align themselves on a self-intersecting curve with complex topological structure.

The book by Mira et al. [9] mentions five examples, including P, of maps with similar properties. They all have in common that the forward iterates seem to form 'folded' chaotic sets, as one can observe in Figure 1. In an attempt to study this behaviour in the simplest possible setting, Garst & Sterk [18, 19] introduced the *fold-and-twist* map. This map produces chaotic sets similar to P, and progress on the fold-and-twist map was made by finding exact expressions for period-3 orbits which seem to extend into chaotic regions, as well as showing the occurrence of a Hopf–Neĭmark–Sacker bifurcation within the parameter plane. However, the question remains as to what is exactly the topological structure of the folded chaotic regions.

One possibility to tackle this problem could be to 'unfold' the chaotic sets, by embedding the non-invertible map into an invertible map of higher dimension, as the paper by Mira [24] outlines. After all, the embedding of the quadratic map $x \longmapsto 1 - ax^2$ into the Hénon map $H_{a,b} : (x, y) \longmapsto (1 - ax^2 + y, bx)$ is exactly of the type described by Mira, and for these maps Benedicks & Carleson [12, 13] famously proved the following. For each $b > 0$ sufficiently close to 0, there exists a set of values of a with positive measure, such that $H_{a,b}$ has a strange attractor which coincides with the closure of the unstable manifold of a saddle fixed point.

In general, *Hénon-like* attractors are said to be the closure of the unstable manifold of a saddle periodic point, and have since been studied and proved to exists in numerous families of maps. The set of orbit points depicted in Figure 1 probably represent an attractor of this type. In fact, Garst & Sterk [18, 19] conjectured that certain attractors of the fold-and-twist map are indeed Hénon-like. This followed after numerically computing the unstable manifolds of

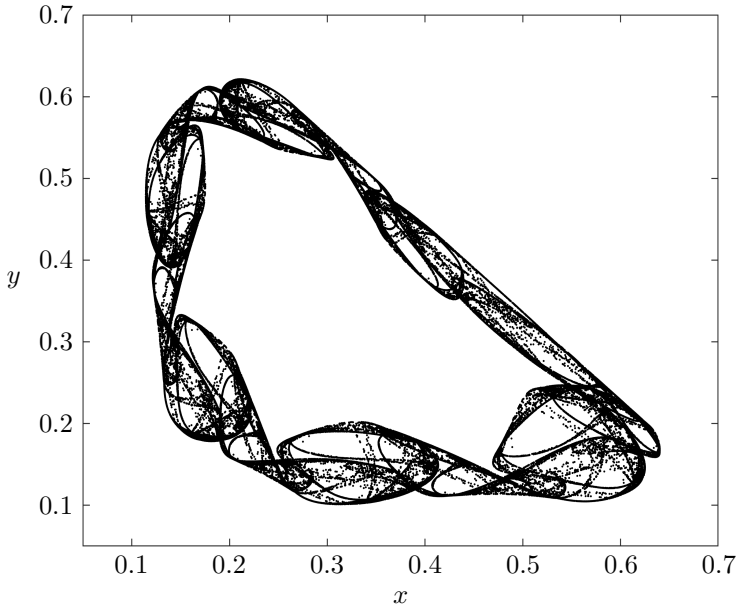

Figure 1: The first 10^4 iterates of the point $(0, 0)$ under the map P, where the parameters are chosen as $a = 3.25$, $b = 3.5$.

continued periodic points, and observing their resemblance to the corresponding attractors, as well as computing a single positive Lyapunov exponent on these attractors. They also asked how this specific structure of the attractors can be proven rigorously. A large portion of our investigation deals with this question, by studying the work of Benedicks & Carleson mentioned earlier.

Finally, a quasi-periodic version of Hénon-like attractors where observed numerically Broer et al. [26] in the Poincaré map of a periodically forced Lorenz-84 model. The attractors they discovered are conjectured to coincide with $\overline{W^u(\mathscr{C})}$ for some quasi-periodic invariant circle $\mathscr{C}$. Therefore, the attractors are named *quasi-periodic Hénon-like* attractors. The same authors later provided rigorous proofs for the existence of such attractors in a certain family of diffeomorphisms of the solid torus, see Broer et al. [16]. This family is a skew product of the Hénon map and the Arnold family of circle maps.

In search of more examples of quasi-periodic Hénon-like attractors, we shall similarly consider a skew product on the solid torus. Specifically, the fold-and-twist map will be coupled to the Arnold map with coupling strength ε. Starting at $\varepsilon = 0$, we shall study whether any of the previously mentioned phenomena occur, and if they persist for $|\varepsilon| \ll 1$.

In order to select appropriate parameter regions for the skew product, we start by studying its individual components. The table of contents reflects the logical structure of the order in which this is done.

2. Objects of study

The first map which we shall briefly investigate is the *Arnold map*. This fairly innocuous looking transformation has been vastly studied since it was first introduced by Arnold [11] in 1961. It has even been applied in biology to study cell cycles and cardiac rhythms, see Glass et al. [27]. To define the map, let the circle be defined as $S^1 = \mathbf{R}/\mathbf{Z}$, and let $\alpha \in [0, 1)$ and $\delta \in \mathbf{R}$ be parameters. When we speak of the Arnold map we mean the family of maps

$$A_{\alpha,\delta} : S^1 \longrightarrow S^1, \quad \theta \longmapsto \theta + \alpha + \delta \sin(2\pi\theta).$$

It is a diffeomorphism of the circle if and only if $0 \leq \delta < \frac{1}{2\pi}$. Moreover, the map $A_{\alpha,\delta}$ is conjugate to $A_{1-\alpha,\delta}$ via the involution $\theta \longmapsto -\theta$. Therefore, we shall usually restrict to the parameters $\alpha \in [0, \frac{1}{2}]$.

The second map which we shall investigate is the the *fold-and-twist map*. The fold-and-twist map is a planar map which has been defined and analysed by Garst & Sterk [18]. It is defined by composing a folding component with a twisting component. Let $a \in [0, 4]$ and $\varphi \in [0, 2\pi)$ be parameters. The folding component is given by the family of quadratic maps

$$F_a : (x, y) \longmapsto (a(\tfrac{1}{4} - x^2) - \tfrac{1}{2}, y).$$

Note that the first component $x \longmapsto a(\frac{1}{4} - x^2) - \frac{1}{2}$ is simply the logistic map $g_a(x) = ax(1 - x)$ shifted to be centred at the origin. The twisting component is given by the counter-clockwise rotation R_φ of φ radians about the origin. The fold-and-twist map is then defined as the family of maps $T_{a,\varphi} = R_\varphi \circ F_a$, or in full

$$T_{a,\varphi} : \begin{pmatrix} x \\ y \end{pmatrix} \longmapsto \begin{pmatrix} \cos\varphi & -\sin\varphi \\ \sin\varphi & \cos\varphi \end{pmatrix} \cdot \begin{pmatrix} a(\frac{1}{4} - x^2) - \frac{1}{2} \\ y \end{pmatrix}.$$

The map $T_{a,\varphi}$ is conjugate to $T_{a,2\pi-\varphi}$ via the involution $(x, y) \longmapsto (x, -y)$, and hence we restrict the parameters to $\varphi \in [0, \pi]$.

The third and final map we shall investigate is a skew product of the first two maps. Broer et al. [16] couple an angular variable to the Hénon map by perturbing its folding component, yielding a map of the solid torus $\mathbf{R}^2 \times S^1$. We now implement the same idea for the fold-and-twist map. Let $\varepsilon \in [-1, 1]$ be a parameter determining the coupling strength. Then, we define the following family of skew products:

$$S : \begin{pmatrix} x \\ y \\ \theta \end{pmatrix} \longmapsto \begin{pmatrix} \begin{pmatrix} \cos\varphi & -\sin\varphi \\ \sin\varphi & \cos\varphi \end{pmatrix} \cdot \begin{pmatrix} (a + \varepsilon \sin 2\pi\theta)(\frac{1}{4} - x^2) - \frac{1}{2} \\ y \end{pmatrix} \\ \theta + \alpha + \delta \sin 2\pi\theta \end{pmatrix}.$$

We shall use the notation S to refer to the above family, without indicating the five parameters $\alpha, \delta, a, \varphi, \varepsilon$ that it depends on. We are interested in S as an example of a map producing quasi-periodic Hénon-like attractors. One difficulty that can be noted immediately, is that the fold-and-twist map is not one-to-one. Therefore, we cannot formally speak of its unstable manifolds, but only its unstable *sets*. Considering the skew product S does not resolve this issue, unfortunately. Likewise, we should expect the attractors of S to feature self-intersections.

3. The dynamics of the Arnold map

To understand a dynamical system, it would be ideal to have explicit access to its evolution map. In the case of the Arnold map, this would mean to exactly compute all iterates of the function

$$A_{\alpha,\delta}(\theta) = \theta + \alpha + \delta \sin(2\pi\theta).$$

However, as with most dynamical systems described by a non-linear map or differential equation, doing these computations in practice is hopeless work. We must therefore resort to general theory.

3.1. Rotation numbers. Let us begin by focusing on the case when the Arnold map is a diffeomorphism of the circle. In this case, the topological dynamics of the map are completely described by the theory of rotation numbers. Here, we outline the main facts needed about rotation numbers; the proofs can be found in for example Brin & Stuck [1].

Any homeomorphism f of the circle can be assigned a unique *rotation number* $\rho(f) \in [0, 1)$. This is done as follows. Let $\pi : \mathbf{R} \longrightarrow S^1$ be the standard covering map. With the covering map, we define a *lift* of f to be a continuous map $F : \mathbf{R} \longrightarrow \mathbf{R}$ such that $\pi \circ F = f \circ \pi$. If F is a lift of f, and $x \in \mathbf{R}$ is any initial point, then it is non-trivial but well known that the limit

$$\rho(F) = \lim_{n\to\infty} \frac{F^n(x)}{n}$$

always exists, and is independent of x. Finally, the *rotation number* of f is defined by the equation $\rho(f) = \pi(\rho(F))$. It holds that $\rho(f)$ is independent of the choice of lift F, and $\rho(f)$ depends continuously on f in the topology of uniform convergence. We shall always choose the unique lift F with $\rho(F) \in [0, 1)$.

We now formulate two propositions describing the dynamics of circle homeomorphisms. The first proposition tells us that if $\rho(f)$ rational, then f has periodic dynamics.

Proposition 3.1. *The rotation number $\rho(f)$ is rational p/q in lowest terms if and only if $F^q(x) = x + p$ for some $x \in \mathbf{R}$, that is, f has a periodic point of minimal period q. In this case, all periodic points have minimal period q, and all other points tend towards one of the periodic orbits.*

The typical case is when all periodic points are hyperbolic. In this case, the circle splits into arcs $[a, b]$, where the endpoints a and b are unstable periodic points, and there exists a single stable periodic point $c \in (a, b)$: it holds that $d(f^n(x), f^n(c)) \to 0$ for all $x \in (a, b)$.

The second proposition tells us that if $\rho(f)$ is irrational, then f has *quasi-periodic* dynamics. Let us quickly explain what this means. Consider the rigid rotation $r_\alpha : \theta \longmapsto \theta + \alpha$ on the circle, where α and *irrational* number. Then each orbit forms a dense set in the circle, so periodic orbits are impossible. Still, the map r_α is *not* chaotic. This is because all orbits are stable: the iterates of any two points always remain equidistant.

Proposition 3.2 (Denjoy's theorem)**.** *Assume f is an orientation preserving C^2 diffeomorphism of the circle. If $\rho(f)$ is irrational, then f is topologically conjugate to the rigid rotation $\theta \longmapsto \theta + \rho(f)$.*

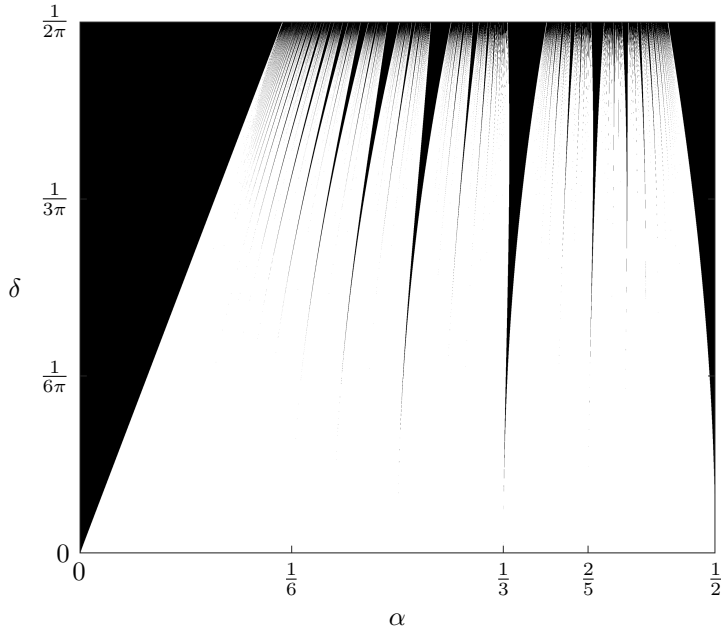

Figure 2: Organisation of the (α, δ) parameter plane for the Arnold map.

The two presented propositions have the following implications for the Arnold map $A_{\alpha,\delta}$. In particular, the organisation of the (α, δ)-plane with respect the dynamics of $A_{\alpha,\delta}$ is of interest. This is studied by considering the continuous function $\tilde{\rho}(\alpha, \delta) = \rho(A_{\alpha,\delta})$. Figure 2 shows the level sets of $\tilde{\rho}$. Each black spike corresponds to the rational value of α which the tip of the spike or reaches at $\delta = 0$. The white area is actually a union of disjoint curves, each of which corresponds to the irrational values of α at $\delta = 0$. However, because the black spikes are so thin near $\delta = 0$, it is impossible to present an clear picture of the irrational curves. See Appendix A.2 for the construction of Figure 2.

The type of spikes observed are a well-known phenomenon of bifurcation diagrams in general, known as *Arnold tongues*. The curves lying in between the tongues are called *hairs*. Let us prove that the tongues and hairs indeed exist. The first step is to observe that for fixed $\delta > 0$, the closed set $\{\alpha \in [0, \frac{1}{2}] : \tilde{\rho}(\alpha, \delta) \text{ is rational}\}$ is an interval with non-empty interior, known as a *periodic interval*. This fact can be shown by using that the Arnold map is an *analytic* map, see Devaney [4]. The second step is to continue the boundary of the periodic intervals in the δ-direction.

Proposition 3.3. *Consider the function $\tilde{\rho}(\alpha, \delta)$ with $\alpha \in [0, \frac{1}{2}]$ and $\delta \in [0, 2\pi]$.*

(i) *For fixed δ, the function $\tilde{\rho}(\cdot, \delta)$ monotonically increases (non-strictly) from 0 to $\frac{1}{2}$.*

(ii) *Each level set of $\tilde{\rho}$ is the closed region lying in between two smooth curves $\alpha = \gamma_1(\delta)$ and $\alpha = \gamma_2(\delta)$.*

Proof. (i) Let $F_\alpha(x) = x + \alpha + \delta \sin(2\pi x)$ be the lift of $A_{\alpha,\delta}$ for $0 \leq \alpha \leq \frac{1}{2}$. Since $F_{\alpha_1}(x) < F_{\alpha_2}(x)$ if $\alpha_1 < \alpha_2$, we have $F^n_{\alpha_1}(x) < F^n_{\alpha_2}(x)$, and so $\rho(A_{\alpha_1,\delta}) \leq$

$\rho(A_{\alpha_2,\delta})$. Now, for $\alpha = 0, \frac{1}{2}$, the point $\theta = 0$ has minimal period $1, 2$ respectively. Then the intermediate value property of $\tilde{\rho}(\cdot, \delta)$ concludes the first part. (ii) To find the curves $\gamma_{1,2}$, note that the points (α, δ) on boundary of a p/q-interval satisfy

$$F^q_{\alpha,\delta}(x) = x + p \quad \text{and} \quad (F^q_{\alpha,\delta})'(x) = 1 \quad \text{for some } x.$$

To solve these equations, we apply the implicit function theorem to the map

$$(\delta, x, \alpha) \quad \longmapsto \quad (F^q_{\alpha,\delta}(x) - x,\ (F^q_{\alpha,\delta})'(x)). \tag{3.1}$$

Let $(a\ \ b; c\ \ d)$ denote the Jacobian of (3.1) in the variables (x, α), then

$$\begin{aligned}
a &= 0, \\
b &= F'_\alpha(F^{q-1}_\alpha(x)) \cdot \partial_\alpha F^{q-1}_\alpha(x) + \partial_\alpha F_\alpha(F^{q-1}_\alpha(x)), \\
c &= \sum_{i=0}^{q-1} \Big[F''_\alpha(F^i_\alpha(x)) \cdot (F^i_\alpha)'(x) \cdot \prod_{j \neq i} F'_\alpha(F^j_\alpha(x)) \Big], \\
d &= \partial_\alpha F'_\alpha(x).
\end{aligned}$$

We need that $bc \neq 0$. Analysing c, we see that $F'_\alpha(y) > 0$ for all y, and $F''_\alpha(y) = -4\pi^2\delta \sin(2\pi y) = 0$ if and only if $y \in \frac{1}{2}\mathbf{Z}$. This happens at consecutive points $y, F_\alpha(y)$ if and only if $\alpha \in \{0, \frac{1}{2}\}$, so $F''_\alpha(F^i_\alpha(x)) \neq 0$ for at least one i. Moreover, all $F''_\alpha(F^i_\alpha(x))$ have the same sign, which shows that $a \neq 0$. For the element b, we have $\partial_\alpha F_\alpha(y) = 1$ for all y. By induction it follows that b is positive for all $q \geq 1$. The implicit function theorem then gives a curve $(x, \alpha) = \gamma(\delta)$ which can be extended to the domain $\delta \in [0, \frac{1}{2\pi}]$, and which solves $(3.1) = (p, 1)$. Projection onto the second coordinate gives curves within the (α, δ)-plane. There might exist such curves crossing the interior of the (p/q)-intervals, but part (i) guarantees that we can take γ_1 as the left-most curve, and γ_2 as the right-most curve.

Herman [20] proved that for fixed δ and any irrational $\rho \in [0, \frac{1}{2}]$, there exists a unique α with rotation number ρ. Thus, the regions with irrational rotation number are single smooth curves, lying in between the periodic intervals. ■

The curves $\gamma_{1,2}$ are curves of saddle-node bifurcation, as the criterion $(F^q_{\alpha,\delta})'(x) = 1$ indicates. To elaborate, fix δ, and imagine that α is increasing. When α hits the left boundary of a periodic-interval, a saddle periodic points appears. As α runs through the interior of the interval, the saddle point splits into a stable and an unstable periodic point, and we are in the hyperbolic case as the remark after Proposition 3.1 describes. When α hits the right boundary, the stable point coalesces with the next unstable point into a single saddle point.

The previous explanation must be nuanced by saying that the bifurcation takes place *within* the periodic interval. When moving outside of the periodic interval, it is *not* the case that quasi-periodic dynamics is simply alternated by periodic dynamics. This becomes clear when considering parameter plane in the line $\delta = 0$: irrational numbers on the real line are not simply alternated by rational numbers. Interestingly, the union of periodic intervals has measure 0 at $\delta = 0$ but increases continuously to full measure $\frac{1}{2}$ at $\delta = \frac{1}{2\pi}$. This is confirmed by Figure 2, where one can observe that the tongues become narrower when δ

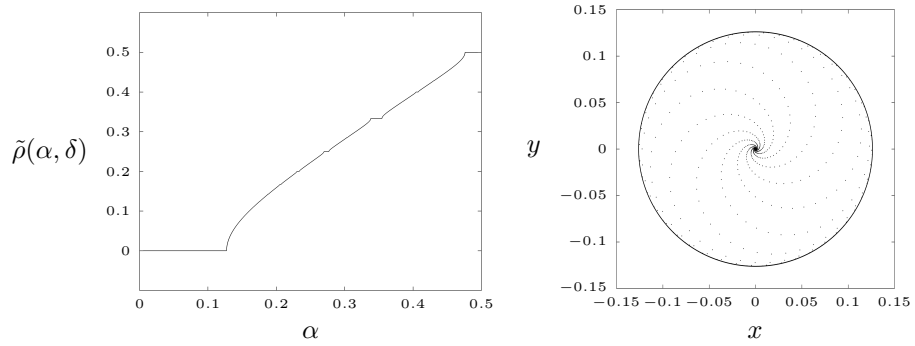

Figure 3: Left: The function $\tilde{\rho}(\cdot, \delta)$ for $\delta = 0.8$. Right: The first 10^4 iterates of the point $(0, 0.0001)$ under the map (3.3) with $\alpha = 0.3778, \delta = \frac{0.1}{2\pi}$. The attracting invariant circle $|y| = \sqrt{\delta}$ can be seen to take shape.

decreases, but also when the denominator of p/q increases. Indeed, past research has found certain laws for the limiting behaviour of $\Delta\alpha = \gamma_2(\delta) - \gamma_1(\delta)$; we now briefly mention a few.

Arnold himself proved that $\Delta\alpha \leq C \cdot \delta^q$ for some constant $C > 0$, and observed that the estimate is sharp in the limit $\delta \to 0$ for fixed q. Ecke et al. [17] noted that Arnold's estimate starts breaking down quickly for values $q \geq 10$. Instead, they provided numerical evidence for the scaling law $\lim_{q\to\infty} q^3 \cdot \Delta\alpha = \text{constant}(\delta)$. In other words, if the period of the dynamics is doubled, then the associated periodic interval shrinks approximately eight-fold. This law was later proved by Jonker [21] to hold for certain families of circle maps, but it is unknown if the Arnold map belongs to these. Jonker's key assumption is that

> on any boundary point of an Arnold tongue, precisely one periodic orbit exists.

If one plots the graph of $A^q_{\alpha,\delta}$ for small q, then this assumption seems to hold true for the Arnold map.

3.2. The Hopf–Neĭmark–Sacker bifurcation. As we shall see later for the fold-and-twist map, Arnold tongues are a typical phenomenon in the parameter plane of maps which contain oscillating components being controlled by two real parameters. For certain parameters, the oscillating components create invariant circles, on which the dynamics alternates between periodic and quasi-periodic. To formalise this, let $\mathscr{M}$ be a (topological) manifold traditionally called the *state space*, and let $f : \mathscr{M} \longrightarrow \mathscr{M}$ be a continuous map. Then, an *invariant circle* $\mathscr{C}$ is the image of some topological embedding $S^1 \longrightarrow \mathscr{M}$ together with the property that $f(\mathscr{C}) \subseteq \mathscr{C}$. Since rotation numbers are invariant under topological conjugation, the dynamics on $\mathscr{C}$ can be fully described by lifting f through the embedding $S^1 \longrightarrow \mathscr{M}$.

If the dimension of $\mathscr{M}$ is at least 2, invariant circles are often born out of periodic points through a so called *Hopf–Neĭmark–Sacker* bifurcation, which is loosely speaking a discrete version of the Hopf bifurcation in flows. The books by Kuznetsov [7] and Broer & Takens [2] contain more details on this bifurcation, but we briefly explain its workings here. Let $f = f_{\beta,\mu}$ be a sufficiently smooth

family of planar maps, where β and μ are real parameters. Initially, suppose that f has a fixed point p of focus type, that is, its two eigenvalues are complex conjugates lying outside of the unit circle. If the eigenvalues cross the unit circle by shifting parameters, an invariant circle $\mathscr{C}$ is born out of p, and the stability of p flips. As the dynamics on $\mathscr{C}$ varies between periodic and quasi-periodic, the Arnold tongues arise in the (β, μ)-plane.

The bifurcation can be expressed in a topological normal form. For $y \in \mathbf{C}$, $\beta \in [0, 1)$, and μ passing through the value 1, the normal form is given by

$$y \longmapsto \mu e^{i\beta} y + \mathscr{O}(|y|^2). \tag{3.2}$$

Here, the terms $\mathscr{O}(|y|^2)$ should contain at least a third-order term. In general, if p is a point with minimal period n, then we say that f undergoes a Hopf–Neĭmark–Sacker bifurcation if f^n does in the previous sense.

While Arnold map is a 1-dimensional map, it can be extended to a 2-dimensional map in the plane in the form of (3.2). In complex notation, the 1-dimensional map takes the form $e^{2\pi i\theta} \longmapsto e^{2\pi i(\theta+\alpha+\delta\sin(2\pi\theta))}$. Then, for $y = |y|e^{2\pi i\theta} \in \mathbf{C}$, we consider the map

$$y \longmapsto (1 + \delta - |y|^2) e^{2\pi i(\alpha+|y|^2\sin(2\pi\theta))} y. \tag{3.3}$$

It can be seen that the circle $|y| = \sqrt{\delta}$ is invariant for this map, and the dynamics on this circle are precisely given by the Arnold map. Besides that, (3.3) satisfies the form (3.2). However, one should take a little care to check the differentiability of terms like $e^{2\pi i|y|^2\sin(2\pi\theta)}y$: it is C^1 in y but not C^2.

Clearly, the invariant circle is asymptotically stable (see Figure 3), and therefore the parameter plane of (3.3) is equal to that in Figure 2. In fact, we have the following proposition, with which be close the paragraph.

Proposition 3.4. *Fix a parameter value $\alpha \in [0, \frac{1}{2}]$ such that $\alpha \neq 0, \frac{1}{2}, \frac{1}{3}, \frac{1}{4}$ to avoid strong resonances. As δ increases through 0, the map* (3.3) *undergoes a supercritical Hopf–Neĭmark–Sacker bifurcation.*

Proof. We follow the theory of Kuznetsov [7]. For any δ, a straightforward calculation shows that the eigenvalues of (3.3) at $y = 0$ are given by $(1+\delta)e^{\pm i\varphi(\delta)}$, where $\varphi(\delta) = 2\pi\alpha$ is a constant function. When $\delta = 0$, the map (3.3) has the form

$$y \longmapsto (1 + \delta)e^{2\pi i\alpha} y + c(0)|y|^2 y,$$

where $c(0) = -e^{2\pi i\alpha}$. The first Lyapunov coefficient is then given by the formula $\mathrm{Re}(e^{-i\varphi(0)}c(0)) = -1$. The proposition then follows from Theorem 4.6 in Kuznetsov [7]. ∎

3.3. The supercritical region. If $\delta > \frac{1}{2\pi}$, then the Arnold map $A_{\alpha,\delta}$ is no longer injective. In this region, the behaviour of the map is more fickle compared to the region $\delta \leq \frac{1}{2\pi}$. Therefore, the regions are labelled as *supercritical* and *subcritical*, respectively.

The unpredictable behaviour in the supercritical region can again be explained with rotation numbers. In general, the rotation number of circle maps which are not one-to-one can still be defined via a lift F and the number $\lim_{n\to\infty} F^n(x)/n$,

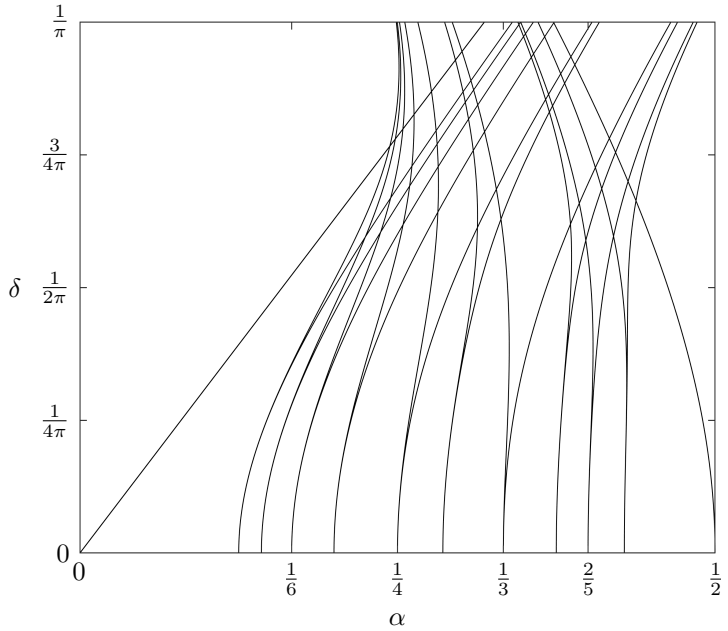

Figure 4: The boundary curves of some resonance tongues in the Arnold map $A_{\alpha,\delta}$. The curves are computed using a Newton method based on the proof of Proposition 3.3.

but this number now depends on the starting point x. However, it is still true that if this limit equals p/q in lowest terms for some x, then there exists a point on the circle with minimal period q.

For the Arnold map, all of this means that the Arnold tongues can be continued into the supercritical region, but the tongues will start to overlap. This phenomenon is illustrated in Figure 4. Inside the overlap of two tongues, two periodic orbits coexist independently of one another. This leads to the view that more and more periodic orbits coexist as more and more tongues overlap. While this is certainly true, it is not the case that all periodic orbits are born out of a saddle-node bifurcation at the tongue boundaries. In special cases, a period-doubling bifurcation and a saddle-node bifurcation take place simultaneously. An example of this mechanism is sketched in Figure 5. We now give a guiding explanation for this figure.

Consider parameters within the (1/2)-tongue such that there is a single stable period-2 orbit (shown in black). Let us now increase δ. If a period-doubling bifurcation occurs, then we have crossed the boundary of the (1/4)-tongue. But as we established the tongue boundaries are curves of saddle-node bifurcation. This means that on the boundary, a saddle period-4 orbit is born (shown in blue), and the stable period-2 orbit turns into a saddle period-2 orbit. Passing the (1/4)-tongue boundary, and the saddle period-4 orbit undergoes a saddle-node bifurcation, and the saddle period-2 orbit undergoes a period-doubling bifurcation.

The period-doubling bifurcation is supported by numerical evidence shown in Figure 6. The figure even shows a cascade of period-doublings, taking place

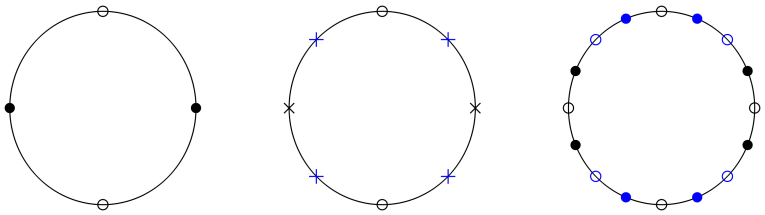

Figure 5: A sketch of a simultaneous saddle-node and period-doubling bifurcation, as δ is increased going from left to right. Symbols: $\bullet$ = stable node, $\circ$ = unstable node, $\times$ = saddle.

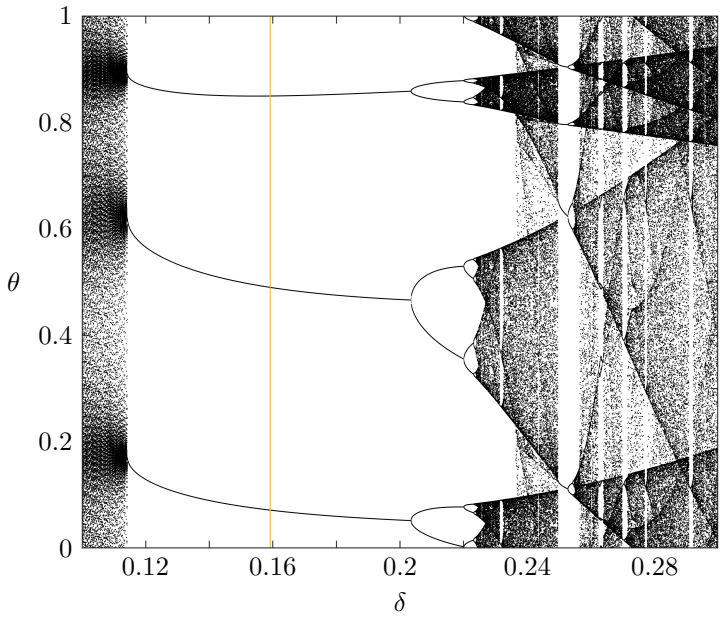

Figure 6: Bifurcation diagram of the Arnold map for $\alpha = 0.35$. The yellow line indicates the critical value $\delta = \frac{1}{2\pi}$.

within the (1/3)-tongue. In turn, this suggests that the Arnold map is chaotic for specific parameters values. However, it is important to note that the cascade is *not* universal in the sense of Feigenbaum, since it has Feigenbaum constant $\delta \approx 2.833$.

All of the facts in this paragraph, together with a much more detailed analysis of the bifurcation behaviour, can be found in the paper by MacKay & Tresser [22].

4. The dynamics of the fold-and-twist map

Recall the fold-and-twist map defined in Section 2:

$$T_{a,\varphi} : \begin{pmatrix} x \\ y \end{pmatrix} \longmapsto \begin{pmatrix} \cos\varphi & -\sin\varphi \\ \sin\varphi & \cos\varphi \end{pmatrix} \cdot \begin{pmatrix} a(\frac{1}{4} - x^2) - \frac{1}{2} \\ y \end{pmatrix}.$$

This is a non-invertible map of a specific type, according to the framework introduced by Mira et al. [23]. There is a *critical line* LC defined by the image set $T_{a,\varphi}(\{(x, y) \in \mathbf{R}^2 : x = 0\})$. Points above this line have no pre-images under $T_{a,\varphi}$, whereas points below this line have precisely two pre-images under $T_{a,\varphi}$. Such maps are said to be of *type* (Z_0, Z_2), and they are studied in general by Mira et al. [23].

4.1. Basins and trapping regions. On the most basic level, we can try to understand the dynamics of the fold-and-twist map by identifying attractors and repellors. These can be detected using trapping regions. Recall that *trapping region* for a map $g : X \longrightarrow X$ is a compact neighbourhood $K \subseteq X$ such that $g(K) \subseteq K$ and $g^n(K) \subseteq \operatorname{int} K$ for some $n \geq 1$. A trapping region defines an attractor as the intersection $\bigcap_{n\geq 0} g^n(K)$.

For the fold-and-twist map $T_{a,\varphi}$, the critical line LC generates a trapping region K by iterating LC a number of times under $T_{a,\varphi}$; see Figure 7 for an example. Basically, all the dynamics of the fold-and-twist map takes place within the region K. Hereby, we mean that there is a basin $\mathscr{D}$ consisting of those points which map to K after a finite number of iterations, while the orbits of points

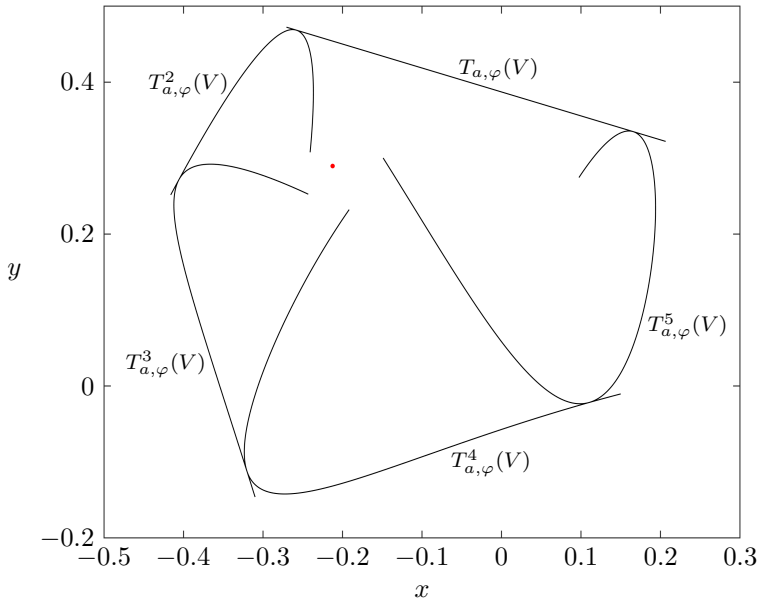

Figure 7: An example trapping region for the fold-and-twist map $T_{a,\varphi}$, where V is a segment of the line $x = 0$. The unstable fixed point (red) is also depicted. Parameters: $a = 3.477$, $\varphi = 72.5°$.

outside of $\mathscr{D}$ are unbounded. Note however that we do not present a strict proof for the existence or shape of $\mathscr{D}$. What we *can* argue, is that

> for all choices of a and φ, there is a number $M > 0$, such that if $\|(x, y)\| \geq M$, then $\|T^n_{a,\varphi}(x, y)\| \to \infty$.

To see this, note that $T_{a,\varphi}$ is norm-decreasing precisely on the set of points $S = \{(x, y) : \frac{1}{2} - \frac{1}{a} \leq |x| \leq \frac{1}{2}\}$, while iterates outside of S increase in norm exponentially. So, if $(x, y) \in S$, then $T_{a,\varphi}(x, y)$ loses norm relative to (x, y). This loss is compensated for by increase in norm of $T^2_{a,\varphi}(x, y)$, provided that $T_{a,\varphi}(x, y)$ lies far enough outside of S. This is achieved by requiring that $|y|$ be large enough for the rigid rotation R_φ to send the point $(0, y)$ to a point with sufficiently large x-coordinate. The exact details are left to the reader.

The basin $\mathscr{D}$ is of interest from the point of view of numerical experiments, since the orbits that remain bounded are the only 'computable' ones. The research by Mira et al. [23] already suggests that exact expressions for boundary of $\mathscr{D}$ are difficult to obtain. On the basis of their research, as well as numerical evidence of Garst & Sterk [18], one can expect $\mathscr{D}$ to be a simply connected, bounded domain of $\mathbf{R}^2$ with a smooth boundary when $a \leq 3$. As a increases past 3, the basin starts to contain holes whose boundaries have a fractal structure. The component of $\mathbf{R}^2 \setminus \mathscr{D}$ which is unbounded may also be viewed as a 'hole'. Eventually, the holes inside $\mathscr{D}$ expand, the boundaries of the holes touch, and $\mathscr{D}$ loses connectivity entirely.

Exact calculations on other aspects of the fold-and-twist map were obtained by Garst & Sterk [18]. These results mainly concern exact expressions for fixed points, points of period three and four, and all their respective stability regions in the parameter plane. Satisfying as exact results may be, they only paint a limited picture of the dynamics of the fold-and-twist map. We therefore turn to analyse the map numerically.

4.2. Lyapunov exponents. Instead of rotation numbers, the main tool for analysing the dynamics of the fold-and-twist map will be Lyapunov exponents. These are numbers which represent the growth of directional derivatives along orbits. Derivatives which grow exponentially fast in the transverse direction of the evolution are often associated with chaotic behaviour. We formalise these ideas briefly.

Lyapunov exponents can be defined for maps and flows on a Riemannian manifold, and even in more general frameworks: see Benettin et al. [14]. Here, we define them for a C^1-smooth map $f : \mathscr{U} \longrightarrow \mathscr{U}$, where $\mathscr{U} \subseteq \mathbf{R}^n$ is an open set. We furthermore assume that $\sup_{x \in \mathscr{U}} \|Df_x\| < \infty$. Choose a point $x \in U$. For any vector $v \in \mathbf{R}^n$, the *Lyapunov exponent* of f in the pair (x, v) is defined as

$$\lambda(x, v) = \limsup_{n \to \infty} \frac{1}{n} \cdot \|Df^n_x(v)\|.$$

With this definition, it is straightforward to show that there is a unique filtration of linear subspaces $V_k \subsetneq V_{k-1} \subsetneq \cdots \subsetneq V_1 = \mathbf{R}^n$, where $k \leq n$ and

(i) for each $i = 1, \ldots, k$, there is a constant λ_i such that $\lambda(x, v) = \lambda_i$ for all $v \in V_i \setminus V_{i+1}$,

(ii) $\lambda_1 > \lambda_2 > \cdots > \lambda_k$.

Colour	Lyapunov exponents	Attractor type
Light blue	$\lambda_2 < \lambda_1 < 0$	Periodic point of node type
Blue	$\lambda_2 = \lambda_1 < 0$	Periodic point of focus type
Green	$\lambda_2 \leq \lambda_1 = 0$	Quasi-periodic invariant circle
Orange	$\lambda_2 \leq 0 < \lambda_1$	Chaotic Hénon-like attractor
Yellow	$0 < \lambda_2 \leq \lambda_1$	Chaotic attractor
Purple		No attractor detected

Table 1: Colour coding for Lyapunov diagrams.

The numbers $\lambda_1, \lambda_2, \ldots, \lambda_k$ are called the *Lyapunov exponents* of f at x. If the vector v is chosen randomly in $\mathbf{R}^n$, then point (i) above implies that $\lambda(x, v) = \lambda_1$ with probability 1. Computer error therefore causes trouble when trying to compute the other exponents $\lambda_2, \ldots, \lambda_k$. A stable algorithm to compute all of the exponents is given in Benettin et al. [15]; we outline the algorithm in Appendix A. The importance of the Lyapunov exponents is that they practically classify the type of attractor to which the orbit of x tends, as well as its stability type. The first two exponents λ_1 and λ_2 already provide a large part of this classification, and for the fold-and-twist map there are no more exponents anyway. The classification is outlined in Table 1.

Although rigorous proofs for the classification may require further conditions on f in general, computing the Lyapunov exponents may point towards related aspects of the dynamics which *can* be proven directly. It is especially helpful to compute a *Lyapunov diagram*. This is a discretised region of the parameter space, where the Lyapunov exponents have been computed for each gridpoint. Based on the computed exponents, each gridpoint is coloured as indicated in Table 1. The colour diagram that emerges often indicates the type of bifurcations occurring when shifting parameters.

One caveat of Lyapunov diagrams is that they depend on the initial point $x \in \mathscr{U}$, which is generally chosen to be the same for all gridpoints of the parameter space. Naturally, it might occur that multiple distinct attractors coexists in a map for the same choice of parameters. Only one of the attractors will be noticed by the Lyapunov exponents. At the same time, shifting parameters possibly causes the orbit of x to be attracted back and forth by the other attractors. This can lead to a fuzzy overlap of colour regions in parts of the Lyapunov diagram.

4.3. Normally hyperbolic invariant circles. The Lyapunov diagram of the fold-and-twist map is shown in Figure 8, where the initial point is $(x, y) = (0, 0)$. (All orbits of $T_{a,\varphi}$ which have been computed in this section have initial point $(x, y) = (0, 0)$.) One feature of the diagram that stands out is the line $a = 3$. Below this line, a stable fixed point of focus type exists. Above this line, Arnold tongues can be seen to emerge, which suggests that the focus point bifurcates outwards to a stable invariant circle via a supercritical Hopf–Neĭmark–Sacker bifurcation. These observations were shown by exact calculations in the paper by Garst & Sterk [18], Propositions 1 and 2.

Let us first concentrate on the (quasi-)periodic region above the line $a = 3$. As suggested before, exact expressions for the invariant circle and any periodic points on it are difficult to obtain. For the special angle $\varphi = 90°$, Garst & Sterk [18] were in fact able calculate these. They give numerical evidence to

show that the invariant circle born at the Hopf–Neĭmark–Sacker bifurcation is persistent for perturbations in φ around 90°. If the the invariant circle at $\varphi = 90°$ was smooth, the theory of normally hyperbolic invariant manifolds treated by Hirsch, Pugh, & Shub [6] would make its persistence rigorous. However, at $\varphi = 90°$ the invariant circle is *not* smooth: it has four corners which coincide with a stable period-4 orbit. Away from the four corners, the invariant circle is normally hyperbolic, as we shall show. To my knowledge, this is not enough to prove persistence, and the current literature does not seem to adequately treat the non-smooth case.

The persistence of hyperbolicity is relevant nonetheless, because it limits the type of bifurcations which can occur on the circle. In particular, we shall see that period-doubling bifurcations occur when increasing the parameter $a \gg 3$. It seems reasonable to assume that normal hyperbolicity implies that the new points with doubled period must appear *on* the invariant circle. After all, if the new points where *outside* the circle, then one their stable directions would point normally away from the circle, which seems impossible if the circle is normally stable at the same time. For the fold-and-twist map, numerical evidence suggests chaotic behaviour is not restricted to a circle, as we shall see in a moment. This implies that normal hyperbolicity is lost when increasing a past some value $a_* > 3$.

So consider the values $\varphi = 90°$, $3 < a < 4$, and their associated saddle period-4 orbit

$$(q, -p_-) \longmapsto (p_-, -q) \longmapsto (q, -p_+) \longmapsto (p_+, -q),$$

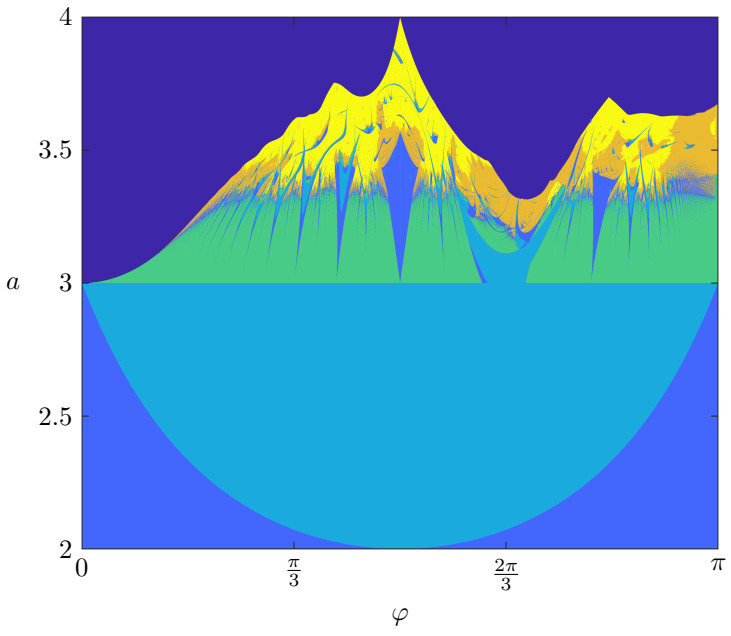

Figure 8: Lyapunov diagram of the fold-and-twist map.

where

$$p_\pm = \frac{-1 \pm \sqrt{(a-3)(a+1)}}{2a} \quad \text{and} \quad q = \frac{2-a}{2a}.$$

The unstable manifold of the point $(q, -p_-)$ is a topological invariant circle $\mathscr{C}$ equal to the square with sides given by the four lines $x = p_\pm$ and $y = -p_\pm$. Alternatively, it is given by the four unstable manifolds of each of the orbit points under the map $T^4_{a,\varphi}$. The following proposition says that $\mathscr{C}$ is r-normally hyperbolic almost everywhere with $r = 4$.

Proposition 4.1. *For all points $(x, y) \in \mathscr{C}$, except its four corners, the tangent space of $\mathbf{R}^2$ at (x, y) splits as*

$$T_{(x,y)}\mathbf{R}^2 = T_{(x,y)}\mathscr{C} + N^s(x, y),$$

where N^s is a piece-wise smooth section of the restricted bundle $T\mathbf{R}^2|_{\mathscr{C}}$, such that

$$\|DT_{a,\varphi}|_{N^s}(x, y)\| < \|DT^4_{a,\varphi}|_{T\mathscr{C}}(x, y)\|.$$

Proof. Suppose first that (x, y) lies on one of the sides $y = -p_\pm$. Then, the Jacobians of $T_{a,\varphi}$ and $T^4_{a,\varphi}$ at (x, y) are given by

$$DT_{a,\varphi}(x, y) = \begin{pmatrix} 0 & -1 \\ -2ax & 0 \end{pmatrix},$$
$$DT^4_{a,\varphi}(x, y) = \begin{pmatrix} 4a^2x(\frac{1}{2} - a(\frac{1}{4} - x^2)) & 0 \\ 0 & 4a^2p_-p_+ \end{pmatrix}.$$

Let $N^s(x, y) = \text{span}\{(0, 1)\}$, while we know that $T_{(x,y)}\mathscr{C} = \text{span}\{(1, 0)\}$. Then, it suffices to check that $\|DT_{a,\varphi}(x, y)(0, 1)\| < \|DT^4_{a,\varphi}(x, y)(1, 0)\|$. Indeed, it is straightforward to find $a_* > 3$ such that $1 < 4a^2|x(\frac{1}{2} - a(\frac{1}{4} - x^2))|$ when $p_- < x < p_+$ and $3 < a < a_*$.

For the case that (x, y) lies on one of the sides $x = p_\pm$, we similarly verify that $|p_\pm| < 2a|y(\frac{1}{2} - a(\frac{1}{4} - y^2))|$ for $-p_+ < y < -p_-$ and $3 < a < a_*$. ∎

4.4. Chaotic attractors. In the regions of Figure 8 where the Arnold tongues overlap, Garst & Sterk [18] numerically detected period-doubling cascades when increasing the parameter $a \gg 3$. However, as suggested before, it seems that in many cases the invariant circle does not survive until the end of the cascade. The chaotic behaviour found at the end of a cascade therefore differs from the standard Arnold map treated in Section 3.

To illustrate this, a few attractors of the fold-and-twist map have been computed in Figure 9 and Figure 11. The computed attractors are indeed situated within the trapping region U defined by the critical line. At a glance, the attractors appear to consist of m many 'components'. Computing the orbit of $T^m_{a,\varphi}$ indeed reveals just one of the components. Moreover, in both Figure 9 and Figure 11 saddle points p of period m are detected, and their corresponding unstable sets have been computed. The unstable sets are computed by iterating a small line segment with midpoint p, which is parallel to the eigenvector of $DT^m_{a,\varphi}(p)$ with real eigenvalue $|\lambda| > 1$.

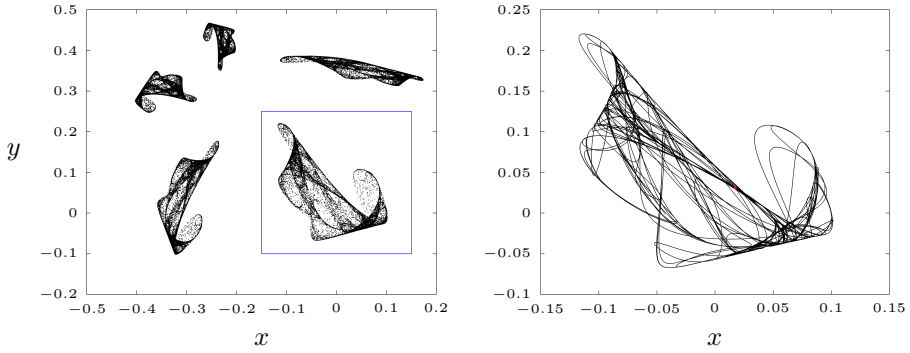

Figure 9: Left: 10^4 iterates of $T_{a,\varphi}$. Right: unstable set of continued period-5 point (red). Parameters: $a = 3.477$, $\varphi = 72.5°$.

The unstable sets are strikingly similar to the computed orbits. Also, on the shown orbits, a single positive Lyapunov exponent is calculated, which corresponds to the orange regions in Figure 8. Note that these regions appear to have positive measure within the parameter plane. These observations suggest that the computed orbits and unstable sets represent a chaotic Hénon-like attractor, and that such attractors occur for a set of parameters with positive measure. We shall use the term *chaotic Hénon-like attractor* to refer to any attractor which satisfies the conclusion of Theorem 7.1, stated later on.

It seems reasonable to suggest that chaotic attractors result from a destruction of the stable invariant circle born of out the Hopf-Neĭmark-Sacker bifurcation. Figure 10 gives an example showing that a single period-doubling bifurcation can already be responsible for such destruction. As mentioned before, it is likely that the circle on the left in Figure 10 is not normally hyperbolic. We note that the period-doubling bifurcation appears to take place in a non-smooth corner of the invariant circle, and large oscillations in the unstable set appear near the corners. For future inquiry, it would be interesting to describe the behaviour of the unstable sets at the bifurcation in detail.

In particular, the unstable sets of the unstable periodic points start to contain self-intersections. We query whether self-intersections in unstable sets are somehow responsible for chaotic behaviour, in similar to the manner to which homoclinic points can cause chaotic behaviour. The answer remains unclear. In Figure 12, a precursor of the attractor within the blue box in Figure 11 is shown. The attractor appears to be Hénon-like without self-intersections, which lies on an unstable curve *with* self-intersections. This would suggest that intersections in unstable sets are unrelated to the (non-)chaoticity of their dynamics. Rather, it seems that a contact bifurcation occurs between basins of the different attractor components when increasing the parameter a, causing the components to merge. In the process, the components meet on the unstable set with self-intersections. An example hereof can be observed between Figure 12 and Figure 11.

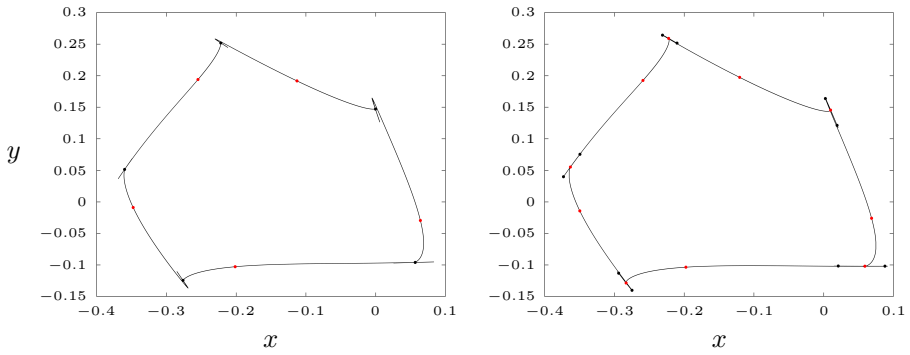

Figure 10: Left: invariant circle of $T_{a,\varphi}$ with stable (black) and unstable (red) period-5 orbit, where $a = 3.33$, $\varphi = 148°$. Right: destruction of invariant circle by period-doubling bifurcation, where $a = 3.35$, $\varphi = 148°$.

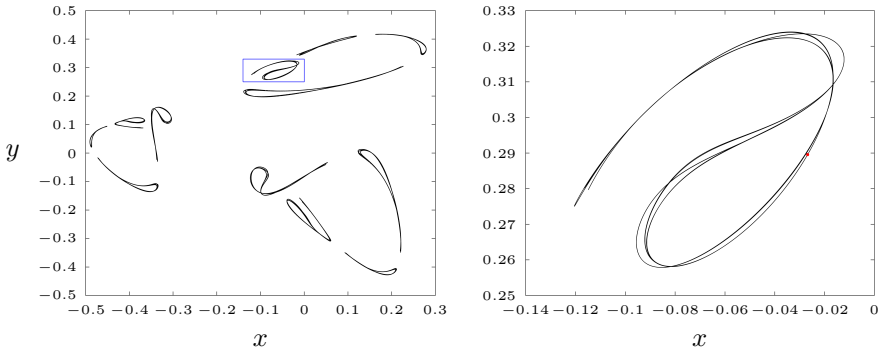

Figure 11: Left: 10^4 iterates of $T_{a,\varphi}$. Right: unstable set of continued period-12 point (red). Parameters: $a = 3.23$, $\varphi = 120°$.

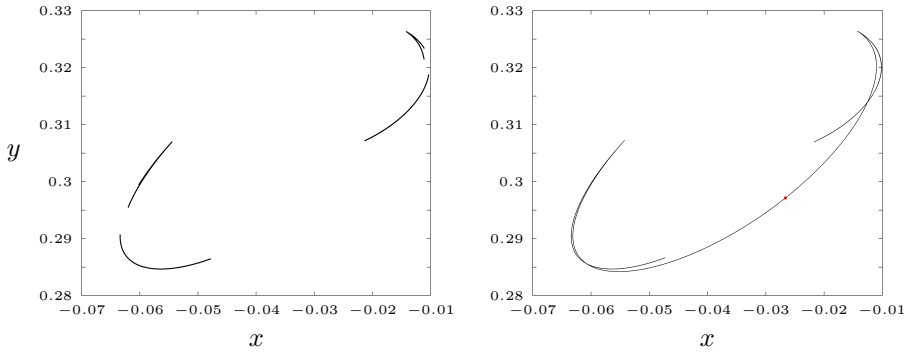

Figure 12: Left: 10^4 iterates of $T_{a,\varphi}$ showing four components of 48-component attractor; the components appear to have no self-intersections. Right: unstable set of a continued period-12 point (red). Parameters: $a = 3.221$, $\varphi = 120°$.

4.5. Multiple unstable directions. Recall that the unstable set of a hyperbolic periodic point p is defined as

$$W^u(p) = \{x \in U : \text{there exists a sequence } (x_i)_{i\in\mathbf{N}} \text{ in } U \text{ such that } \\ x_1 = x,\ f(x_{i+1}) = x_i \text{ for all } i \in \mathbf{N},\ \text{and } \|x_i - f^i(p)\| \to 0\}.$$

At first thought, the possibility that $W^u(p)$ contains a self-intersection seems incongruous, for then multiple unstable directions exist at the intersection point. This section presents a short example to show that this can be the case nevertheless. The example also serves to illustrate possible local dynamics near intersection points.

Consider the map of circle given by the function f shown in Figure 13. The map has a repelling fixed point at $\theta = 0$, an attracting fixed point at $\theta = \frac{1}{2}$, and two saddle fixed points at $\theta = \frac{1}{4}, \frac{3}{4}$. It is clear that $W^u(0) = S^1$.

We now map the circle continuously onto a lemniscate as follows. Identify the circle with the unit circle in $\mathbf{R}^2$ via $\theta \longmapsto e^{2\pi i\theta}$, and apply the transformation $(x, y) \longmapsto (x, xy)$. The image of the unit circle under this transformation will form a lemniscate L, say, whereby the points $\theta = \frac{1}{4}, \frac{3}{4}$ are mapped onto the intersection point. The map f therefore induces a map on L, for which it holds that $W^u(0) = L$. Thus, the unstable set perfectly well contains a self-intersection.

It is plain to embed this map within in a smooth map of $\mathbf{R}^2$. Consider the collection of circles foliating $\mathbf{R}^2$, and define appropriate circle maps that 'fill in' the dynamics of f, while remembering that the points $\theta = \frac{1}{4}, \frac{3}{4}$ need to remain fixed. Straightforward perturbations of f will do the trick.

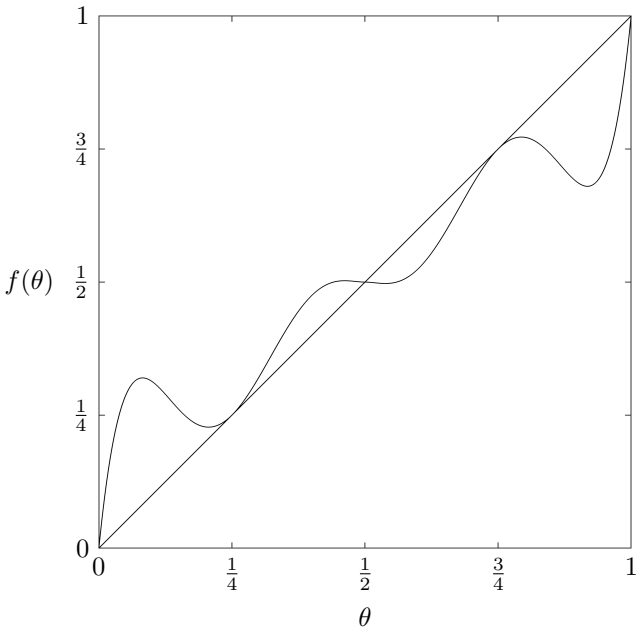

Figure 13: A circle map represented by a function f on the interval [0,1]. The function f is a cutting and pasting of the polynomial $32x^5 - 60x^4 + 32x^3 - 3x^2$.

5. The dynamics of the skew product: a phenomenological analysis

Recall the family of skew products S of the fold-and-twist map and the Arnold map defined in Section 2:

$$S : \begin{pmatrix} x \\ y \\ \theta \end{pmatrix} \longmapsto \begin{pmatrix} \begin{pmatrix} \cos\varphi & -\sin\varphi \\ \sin\varphi & \cos\varphi \end{pmatrix} \cdot \begin{pmatrix} (a + \varepsilon \sin 2\pi\theta)(\frac{1}{4} - x^2) - \frac{1}{2} \\ y \end{pmatrix} \\ \theta + \alpha + \delta \sin 2\pi\theta \end{pmatrix}.$$

The family S can be put into the following framework, introduces by Broer et al. [16]. Fix a smooth map $K : \mathbf{R}^2 \longrightarrow \mathbf{R}^2$, as well as a smooth family of maps $P_\varepsilon : \mathbf{R}^2 \times S^1 \longrightarrow \mathbf{R}^2 \times S^1$ depending on a parameter $\varepsilon \in [-1, 1]$. Recall that $A_{\alpha,\delta} : S^1 \longrightarrow S^1$ denotes the Arnold map, and consider the family

$$(K, A_{\alpha,\delta}) + P_\varepsilon : \mathbf{R}^2 \times S^1 \longrightarrow \mathbf{R}^2 \times S^1. \tag{5.1}$$

The family S can be put in this form: take has $K = T_{a,\varphi}$ and $P_\varepsilon(x, y, \theta) = (R_\varphi(\varepsilon \sin 2\pi\theta \cdot (\frac{1}{4} - x^2), 0), 0)$. For such families, Broer et al. [16] prove various theorems on the existence of Hénon-like attractors for sets of parameters with positive measure. However, all their proofs assume that the map K is *dissipative*: $|\det DK(x, y)| < 1$ for all $(x, y) \in \mathbf{R}^2$. This is not the case for the fold-and-twist map; it has a Jacobian given by

$$DT_{a,\varphi}(x, y) = \begin{pmatrix} \cos\varphi & -\sin\varphi \\ \sin\varphi & \cos\varphi \end{pmatrix} \cdot \begin{pmatrix} -2ax & 0 \\ 0 & 1 \end{pmatrix},$$

and hence $|DT_{a,\varphi}(x, y)| = 2a|x|$. When looking at Figure 7, it is quite evident that the fold-and-twist map is area expanding even within the small domain where the attractors occur.

One would like to analyse the dynamics of the family S nonetheless, especially the dependence on the coupling strength ε. For this, we again make use of Lyapunov diagrams. Note that all orbits are computed with initial point $(x, y, \theta) = (0, 0, 0)$.

Also note the third component of the skew product S: it is decoupled from the other components. Therefore, it is convenient to distinguish between the case when the Arnold map has periodic dynamics, and when it has quasi-periodic dynamics. In Figure 14, Lyapunov diagrams have been computed for either case.

5.1. Case 1: the Arnold map is periodic. Fix $\{\theta_i\}$ as a stable orbit of period q for the Arnold map, and let $\mathscr{A}$ be an attractor of the fold-and-twist map. Suppose first that $\varepsilon = 0$. Then the Lyapunov diagram of S is identical to the Lyapunov diagram of $T_{a,\varphi}$ (see Figure 8). This is because the orbit $\{\theta_i\}$ is stable, so any attractor of S is now a subset of the disjoint union $\{\theta_i\} \times \mathscr{A}$. The dynamics of S on $\mathscr{A} \times \{\theta_i\}$ will be an iterate of the dynamics of $T_{a,\varphi}$ on $\mathscr{A}$. In particular, the Hopf–Neĭmark–Sacker bifurcation still occurs for $\varepsilon = 0$, albeit now q stable invariant circles bifurcate out of a periodic orbit.

When $0 < |\varepsilon| \ll 1$, the Lyapunov diagram in Figure 15 indicates the persistence of all types of attractor $\mathscr{A} \times \{\theta_i\}$, as well as persistence of the Hopf–Neĭmark–Sacker bifurcation. When $\mathscr{A}$ is periodic or quasi-periodic, the

persistence can be shown rigorously using the the theory of normally hyperbolic invariant manifolds, see for example Hirsch, Pugh & Shub [6]. However, this theory is not adequate enough to prove the persistence of the Hopf–Neĭmark–Sacker bifurcation, although we provide further evidence for the persistence in a bifurcation diagram, see Figure 19.

More importantly, if $\mathscr{A}$ is chaotic Hénon-like attractor, the question is whether taking $0 < |\varepsilon| \ll 1$ generates a perturbed version of $\mathscr{A} \times \{\theta_i\}$ which is also chaotic Henón-like. Broer et al. [16] proved such persistence in product maps of the form (5.1), where K is a dissipative map, for example the Henón map. Our computations for the fold-and-twist skew product show that the orange regions in Figures 14 and 15 corresponding to one positive Lyapunov exponent appear to have positive measure, including for $|\varepsilon| \ll 1$. Therefore, if Hénon-like attractors can be proved to exists in the fold-and-twist map, then the arguments used by Broer et al. may apply to the skew product S as well.

5.2. Case 2: the Arnold map is quasi-periodic. Again, first suppose there is no coupling in S: $\varepsilon = 0$. In this case, the Lyapunov diagram of S is again identical to the diagram of $T_{a,\varphi}$, except that any periodic regions have now turned into quasi-periodic regions. This situation is dual to the one described in the previous paragraph: if $\{p_i\}$ is a stable periodic orbit of $T_{a,\varphi}$, then $\{p_i\} \times S^1$ is a stable union of invariant quasi-periodic circles, which are persistent under small perturbations of ε. An example of such a union of circles depicted in Figure 16.

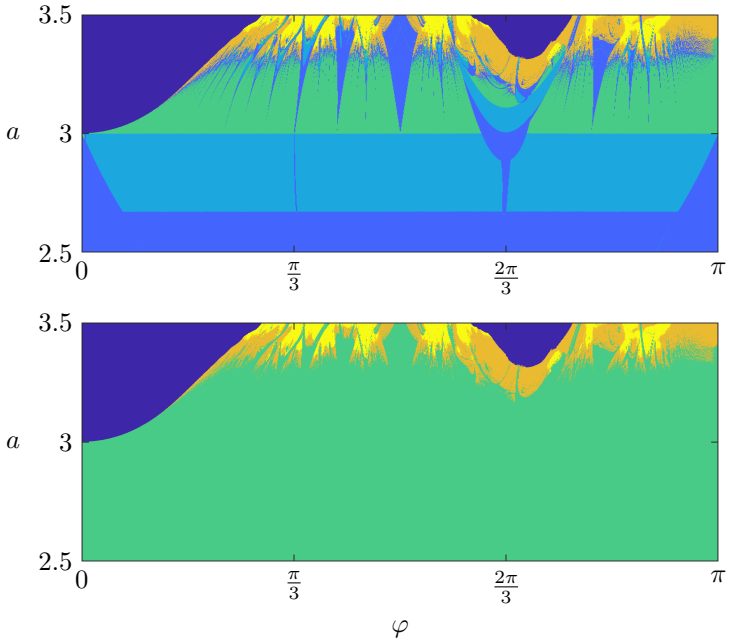

Figure 14: Lyapunov diagrams the skew product S with non-trivial coupling $\varepsilon = 0.01$. Top: $\alpha = 0.35$, $\delta = \frac{0.8}{2\pi}$ (period-3 Arnold dynamics). Bottom: $\alpha = 0.36$, $\delta = \frac{0.8}{2\pi}$, (quasi-periodic Arnold dynamics).

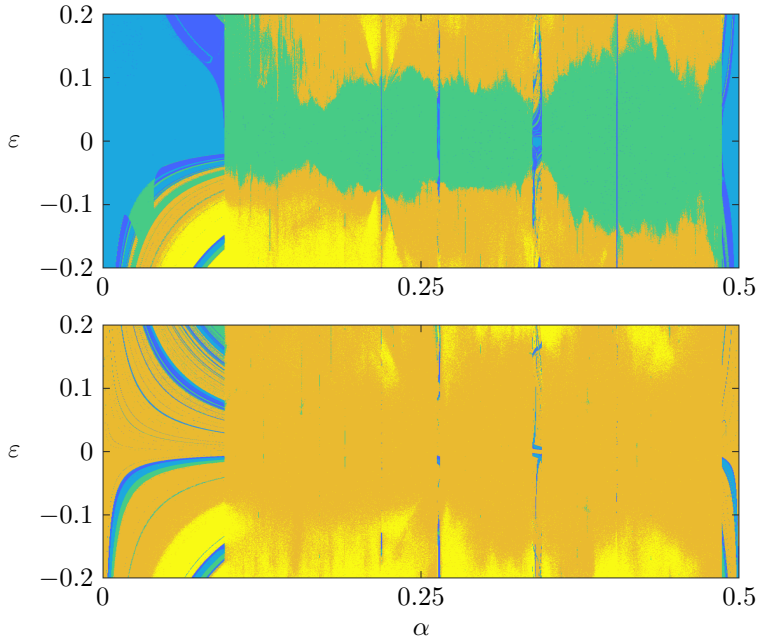

Figure 15: Lyapunov diagrams for the family S with $\delta = 0.6/2\pi$. Top: $a = 3.4$, $\varphi = 74°$ (periodic fold-and-twist dynamics). Bottom: $a = 3.5$, $\varphi = 95°$ (chaotic Hénon-like fold-and-twist dynamics). Some sharp vertical cut-off lines can be noted, as a result of moving through the Arnold tongues of the Arnold map in the horizontal direction.

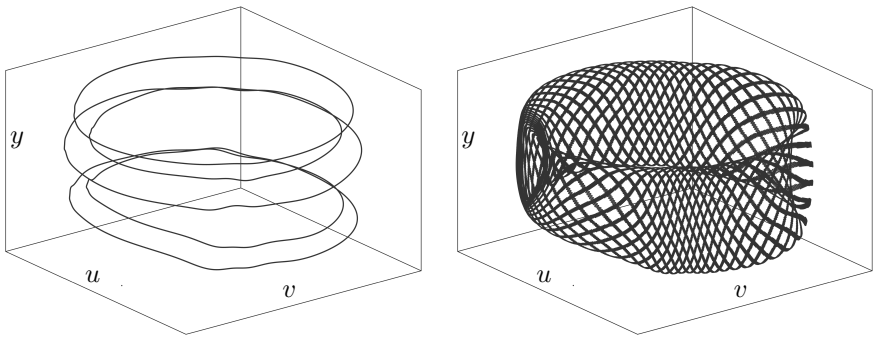

Figure 16: Left: a union of stable quasi-periodic invariant circles as an attractor for S, where $a = 3.1$, $\varphi = 72.5°$, $\alpha = 0.36$, $\delta = \frac{0.8}{2\pi}$, and $\varepsilon = 0.1$. Right: the same parameters as the left except $\varphi = 74°$; there appears to be an invariant torus containing a union of invariant circles as the attractor of S. Projection on the (u, v, y)-space, where $u = (x - 1)\cos(2\pi\theta)$, $v = (x - 1)\sin(2\pi\theta)$.

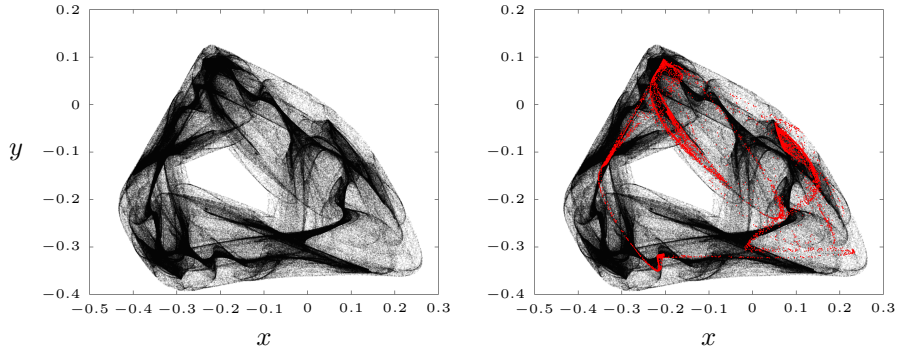

Figure 17: Left: attractor of S projected on the (x, y)-plane, where $a = 3.39$, $\varphi = 148°$, $\alpha = (\sqrt{5}-1)/2$, $\delta = 0$, and $\varepsilon = 0.1$. Right: the same attractor, where orbit points within the slice $0.24 < \theta < 0.25$ have been coloured red.

Next, it is possible the attractor $\mathscr{A}$ of $T_{a,\varphi}$ itself is a union of stable invariant circles. This does not occur for the Hénon map, this case is therefore not studied by Broer et al. [16]. Calculating orbits of such cases shows that an invariant torus exists for the skew product, see Figure 16, which is persistent in perturbations of ε. This suggests that a hyperbolic torus bifurcates out of the invariant circle $\{F\} \times S^1$ in a Hopf–Neĭmark–Sacker-like fashion, where F is the stable fixed point of the fold-and-twist map in the regime $a < 3$, and $\varepsilon = 0$. Of interest would be the dynamics on this torus on the basis of the fraction of rotation numbers $\rho(T_{a,\varphi}|_{\mathscr{A}})/\rho(A_{\alpha,\delta})$ being rational or irrational. The framework of *multi-periodic subsystems* described by Broer & Takens [2] (see Definition 2.7) could be helpful. In the rational case, one would expect the torus to contain an attractor which is a union of invariant circles. An example of such a torus is given in Figure 16.

Lastly, we observe that an invariant circle on such a torus can possibly lead to quasi-periodic Hénon-like attractor. An example of such an invariant circle and attractor is shown in Figure 17 and Figure 18. Specifically, we conjecture that these attractors are of the form $\overline{W^u(\mathscr{C})}$, where $\mathscr{C}$ is a quasi-periodic invariant circle of saddle type. Evidence for this is provided by considering slices of the attractor in the θ-direction. The slices reveal a geometric structure akin to the original attractors of $T_{a,\varphi}$, suggesting the the the dynamics on the entire attractor is 'Hénon-like times quasi-periodic'.

Relying again on dissipativity, Broer et al. [16] proved that the attractor in the map (5.1) are quasi-periodic Hénon-like attractors for $\varepsilon = 0$. They conjecture that such attractors persist under small perturbations of ε, after numerically observing sets of parameters with positive measure corresponding to a single positive Lyapunov exponent. Our results for the skew product S suggest likewise results, provided that the attractors in the fold-and-twist map $T_{a,\varphi}$ are indeed Hénon-like.

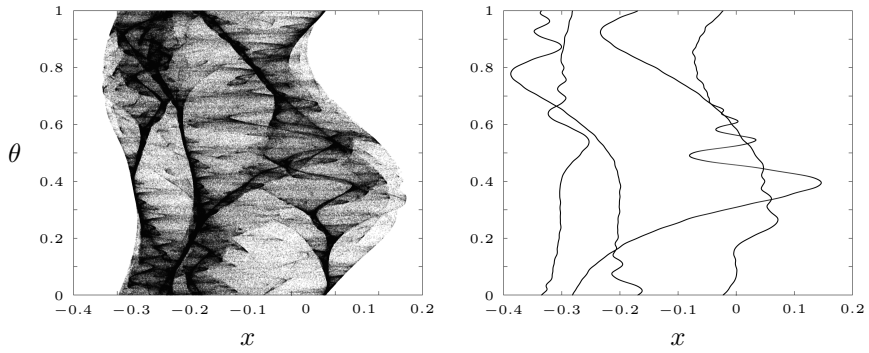

Figure 18: Left: the same attractor as in Figure 17, but projected onto the (x, θ)-plane. Right: the same parameters as the left except $a = 3.27$; the attractor appears to be a single quasi-periodic invariant circle.

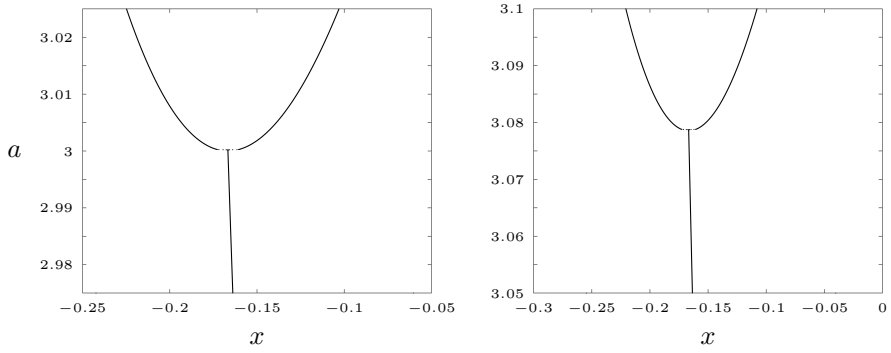

Figure 19: Bifurcation diagrams of the family S, for $\varphi = 148°$, $\alpha = 0.1$, and $\delta = \frac{0.8}{2\pi}$ (the Arnold has a fixed point); as a increases, a stable fixed points bifurcates outwards into a stable invariant circle, whose outermost x-coordinates are shown. Left: $\varepsilon = 0$. Right: $\varepsilon = 0.1$.

6. The dynamics of the quadratic map

As noted earlier, the computed Lyapunov diagram for the fold-and-twist map suggests that its attractors are Hénon-like for a set parameter values with positive measure. This raises the interest in constructing a rigorous proof for their existence. Benedicks & Carleson [13] were among the first to provide such a proof in the case of the Hénon map. With the aim of drawing an analogy between the Hénon map and the fold-and-twist map, we hereby attempt to understand their work in more depth.

The Hénon map $(x, y) \longmapsto (1 - \mu x^2 + y, \nu x)$ may be viewed as a perturbation of the map $x \longmapsto 1 - \mu x^2$, for small $\nu > 0$. As such, it is natural to first analyse $x \longmapsto 1 - \mu x^2$ (see Benedicks & Carleson [12]). In our case, the fold-and-twist map may be viewed as a perturbation of the quadratic map $f_a(x) = a - 1 - ax^2$, where $a \in [0, 2]$. The quadratic map is conjugate to $x \longmapsto 1 - \mu x^2$ for $a, \mu = 2$, and hence the analysis of both maps is similar. Evidently, we shall focus our attention on f_a, and to this end we follow the approach of De Melo & Van Strien [8]. However, De Melo and Van Strien develop a theory applicable to a more general class of maps. The proofs by Benedicks and Carleson are often shorter, yet highly specific to the map $x \mapsto 1 - \mu x^2$. We shall try to find a middle road between the two.

The important property of Hénon-like attractors $\mathscr{A}$ of a smooth map f that we shall focus on is the *Collet–Eckmann condition*: there exists a point $x \in \mathscr{A}$ a unit vector v and a positive constant γ such that $\|Df_x^n(v)\| \geq e^{\gamma n}$ for all $n \geq 0$. The condition implies that the attractor itself contains no periodic attractors. The reason that $1 - \mu x^2$ is nice to work with for $\mu \approx 2$ is that $f_2 : x \longmapsto 1 - 2x^2$ fully conjugate to the tent map $T : x \longmapsto 1 - 2|x|$. From this it quickly follows that f_2 is Collet–Eckmann with $\gamma = \log(2)$ (see Proposition B.2).

The important result by Benedicks and Carleson we shall discuss now, is that a large class of perturbations of f_2 is also Collet–Eckmann with a uniform exponent γ. Before stating their result, we introduce some notation. Let $\xi_0 = 0$ be the unique critical point of each f_a. We denote the iterates of the critical point by $\xi_n(a) = f_a^n(0)$. If the parameter value is fixed and clear from context, we often drop it from the notation and write ξ_n. At the same time, we often see ξ_n as a map $[0, 2] \longrightarrow [-1, 1]$.

Theorem 6.1 (Benedicks and Carleson)**.** *There exists a constant $\gamma > 0$ and a set $E \subseteq [0, 2]$ of positive Lebesgue measure containing the value 2 as a density point, such that for all $a \in E$, it holds that*

$$|Df_a^n(\xi_1)| \geq e^{\gamma n} \qquad \text{for all } n \geq 1.$$

6.1. Preliminary facts and definitions. We shall reserve the symbol $D = \partial_x$ purely for spatial derivatives. Not only the spatial derivatives $\partial_x f_a^k$, but also the parameter derivatives $\partial_a f_a^k$ play an important role in the proof of Theorem 6.1. By the chain rule, we have the two formulas

$$\begin{aligned} \partial_x(f_a \circ f_a^k)(x) &= -2af_a^k(x) \cdot \partial_x f_a^k(x), \\ \partial_a(f_a \circ f_a^k)(x) &= -2af_a^k(x) \cdot \partial_a f_a^k(x) + 1 - (f_a^k(x))^2. \end{aligned} \tag{6.1}$$

These formulas generalise to the following expressions, which we shall make full use of in the upcoming proposition

$$\partial_x f_a^k(x) = \prod_{i=0}^{k-1} -2af_a^i(x), \tag{6.2}$$

$$\begin{aligned}\partial_a f_a^k(x) &= \partial_x f_a^k(x) \cdot \frac{1-x^2}{-2ax} \cdot \prod_{i=1}^{k-1} \frac{\partial_a f_a^{i+1}(x)}{-2af_a^i(x) \cdot \partial_a f_a^i(x)} \\ &= \partial_x f_a^{k-1}(f(x)) \cdot (x^2-1) \cdot \prod_{i=1}^{k-1} \left(1 + \frac{(f_a^i(x))^2 - 1}{2af_a^i(x) \cdot \partial_a f_a^i(x)}\right).\end{aligned} \tag{6.3}$$

(To see the formula for $\partial_a f_a^k(x)$, first telescope using (6.2), and then use (6.1).) From here we will quickly show Proposition 6.4, which is the real starting point towards proving Theorem 6.1

Before this, we make a few more remarks. A smooth map of the interval is called *Misiurewicz* if the forward orbit of any critical point does not cluster at any of the critical points. Proposition 6.5 will imply that if f_a is Misiurewicz then conclusion of Theorem 6.1 holds for a. Although it is trivial that f_2 is Misiurewicz, there are no proofs for general values of $a < 2$. Instead, Benedicks and Carleson constructed a set E of a-values satisfying weaker conditions, but which still imply the conclusion of Theorem 6.1. Actually the set E is very small, it sits very close to 2, and it cannot be given a very concrete description, but it has a Cantor-like structure.

The proof of Theorem 6.1 is broken down into stages. The first stage is to introduce two conditions BA and FA on parameter values a which, when satisfied, guarantee the desired exponential growth of the spatial derivative. The second stage is to show that the set of a-values for BA and FA fail is very small. Most steps along the way rely on constructing partitions of the relevant sets, and analysing all pieces separately.

We now begin by showing the following curious proposition, which shall be used at many stages. It says that *if* the growth of $Df_a^k(\xi_1)$ is exponential, then the parameter and space derivatives are of the same order.

Proposition 6.2. *Suppose $K > 0$, $\gamma > 0$, and $N_0 \geq 1$ are such that $\sum_{k=N_0}^{\infty} e^{-\gamma k} \leq K$. Then there exists $a_0 < 2$ such that if $a \in [a_0, 2]$, $n \geq N_0$, and $|\partial_x f_a^k(\xi_1)| \geq e^{\gamma k}$ for $k = N_0, \ldots, n-1$, then*

$$1 - K \leq \frac{|\partial_a f_a^k(\xi_0)|}{|\partial_x f_a^{k-1}(\xi_1)|} \leq 1 + K \qquad \text{for all } k = N_0, \ldots, n.$$

Proof. The equalities (6.2) and (6.3) show that $|\partial_a f_2^k(\xi_0)|/|\partial_x f_2^{k-1}(\xi_1)| = 1$ as well as

$$\left| \frac{\partial_a f_a^k(\xi_0)}{\partial_x f_a^{k-1}(\xi_1)} - \frac{\partial_a f_a^{k-1}(\xi_0)}{\partial_x f_a^{k-2}(\xi_1)} \right| = \frac{|1 - (f_a^{k-1}(\xi_0))^2|}{|\partial_x f_a^{k-1}(\xi_1)|}.$$

By the exponential growth hypothesis, it follows that

$$\left| \frac{\partial_a f_a^k(\xi_0)}{\partial_x f_a^{k-1}(\xi_1)} - \frac{\partial_a f_a^{N_0}(\xi_0)}{\partial_x f_a^{N_0-1}(\xi_1)} \right| \leq K.$$

Combining this with the fact that $|\partial_a f_2^{N_0}(\xi_0)|/|\partial_x f_2^{N_0-1}(\xi_1)| = 1$, a continuity argument yields $a_0 < 2$ to fulfil the conclusion of the proposition. ■

We now partition the x-space $I = [-1, 1]$ as follows. Introduce neighbourhoods $U_r = (-e^{-r}, e^{-r})$ for $r \in \mathbf{N}$. For the rest of the section, Δ will denote an integer, and we fix the notation $U = U_\Delta$. Set $I_r = U_r \setminus U_{r+1}$, and further partition the left and right components of I_r into r^2 equal parts $I_{(r,-r^2)}, \dots, I_{(r,-1)}, I_{(r,1)}, \dots, I_{(r,r^2)}$. It does not really matter whether these sub-intervals are chosen closed- or open-ended, all that matters is that they are disjoint with equal length $|I_{r,\ell}| = (e^{-r} - e^{-(r+1)})/r^2$.

We also introduce a neighbourhood $W = W_\delta = (-\delta, \delta)$ for some $\delta > 0$ independent of Δ, but in general we pick Δ such that $U_\Delta \subseteq W$.

Definition 6.3. The following terminology implicitly depends on the neighbourhood $U = U_\Delta$. An integer ν is called a *return* for a parameter value a if $\xi_\nu(a) \in U$. The *first free return* (possibly infinity) for a is defined as

$$\nu_1(a) = \inf\{k > 0 : \xi_k(a) \in U\}.$$

It may indeed happen that some parameter values have no finite returns. For instance, $f_2^n(0) = -1$ for all $n \geq 2$. In fact, this particular example implies part (i) of the following most fundamental proposition.

Proposition 6.4. *Suppose $N \geq 2$. For all Δ sufficiently large and all $a_1 < 2$ sufficiently close to 2, there exist $a_0 \in [a_1, 2]$ and an integer $m \geq N$ such that*

(i) *$f_a^i(U_\Delta) \subseteq [-1, -\frac{1}{2}]$ for all $i = 2, \dots, N$ and all $a \in [a_1, 2]$;*

(ii) *The map $\xi_k : [0, 2] \longrightarrow I$ maps $[a_0, 2]$ strictly decreasing onto $[-1, \xi_k(a_0)]$ for $k = 2, \dots, m + 1$;*

(iii) *$\xi_k(a_0) \leq -\frac{1}{2}$ for $k = 2, \dots, m$, but $\xi_{m+1}(a_0) \geq \frac{1}{3}$.*

Proof. (i) By continuity, for all $i = 2, \dots, N$, we may choose $b_i < 2$ and $\Delta_i > 0$ such that $f_a^i(U_{\Delta_i}) \subseteq [-1, -\frac{1}{2}]$ for all $a \in [b_i, 2]$. Then any $\Delta \geq \max \Delta_i$ and $a_1 \geq \max b_i$ have the required properties. (For $i = 2$ we already must have $e^{-\Delta_i} < \frac{1}{3}$ and $b_i > 1.8$.) (iii) A simple computation shows that when $\xi_i \leq -\frac{1}{2}$, we have the inequality

$$\xi_{i+1} - \xi_i = (1 + \xi_i)(a - 1 - a\xi_i) \geq (1 + \xi_i)(2 - \frac{3}{2}(2 - a)).$$

This shows that $1+\xi_i$ grows exponentially as long as $\xi_i \leq -\frac{1}{2}$, hence $\xi_m(a_1) > -\frac{1}{2}$ for some minimal $m \geq 2$. By part (i) it holds that $m \geq N$. Since $\xi_m(2) = -1$, the intermediate value theorem allows us to choose $a_0 \in [a_1, 2]$ such that $\xi_m(a_0) = -\frac{1}{2}$. By the previous inequality, this gives

$$\xi_{m+1}(a_0) \geq -\frac{1}{2} + (1 - \frac{1}{2})(2 - \frac{3}{2}(2 - a_0)) \geq \frac{1}{3}.$$

(ii) If $k \leq m$, then since $\partial_x f_a^k(\xi_1) = \Pi_{i=1}^k -2a\xi_i$ with $|\xi_i| \geq \frac{1}{2}$, we may apply Proposition 6.2 with $\gamma = \log(1.8)$ and $N_0 = 2$. Then for all $a \in [a_0, 2]$ and $k = 2, \dots, m + 1$, it holds that

$$|\partial_a f_a^k(\xi_0)| \geq \frac{1}{4} \cdot |Df_a^{k-1}(\xi_1)| \geq \frac{1}{4} \cdot e^{\gamma k}.$$

By continuity, this implies that $\partial_a f_a^k(\xi_0)$ is strictly positive for all $a \in [a_0, 2]$, or strictly negative for all $a \in [a_0, 2]$. By induction, $\partial_a f_2^k(\xi_0) < 0$ for all $k \geq 2$, so the latter is the case. ■

For proving Theorem 6.1, the previous lemma allows us to reduce to iterates $n \geq N$, and find $E \subseteq [a_0, 2]$. Namely, the proof for part (ii) of the lemma implies that for any $N \geq 1$ and $\gamma < \log 2$, we may choose $a_0 < 2$ such that $|Df_a^k(\xi_1)| \geq e^{\gamma k}$ for all $a \in [a_0, 2]$ and $k = 1, \ldots, N$. The following proposition generalises this fact, and will be used to obtain exponential growth after time N.

Proposition 6.5. *For all $\delta \in (0, \frac{\sqrt{5}-1}{4})$, there exists a constant $C_0 > 0$ such that the following holds. For all $\gamma_0 < \log(2)$ and all neighbourhoods $U_\Delta \subseteq W_\delta$, there exists $a_0 < 2$ such that for all $a \in [a_0, 2]$ and $k \geq 0$, we have*

(i) *if $f_a^j(x) \notin W_\delta$ for $0 \leq j \leq k-1$, then*

$$|Df_a^k(x)| \geq C_0 \cdot e^{\gamma_0 k},$$

(ii) *if $f_a^j(x) \notin U_\Delta$ for $0 \leq j \leq k-1$, then*

$$|Df_a^k(x)| \geq C_0 \cdot e^{\gamma_0 k} \cdot \inf_{0 \leq j \leq k-1} |f_a^j(x)|,$$

(iii) *if $f_a^j(x) \notin U_\Delta$ for $0 \leq j \leq k-1$ and $f_a^k(x) \in W_\delta$, then*

$$|Df_a^k(x)| \geq e^{\gamma_0 k}.$$

Proof. Suppose that the proposition is true for the maps $g_a : x \longmapsto 1 - ax^2$ (still $a \leq 2$, $x \in I$). Then the the proposition is also true for f_a with the same δ and γ_0, but modified C_0 and a_0. Namely, observe that the interval $[1-a, a-1]$ is f_a-invariant, and in fact $f_a|_{[1-a,a-1]}$ is precisely a dilation of g_a. Hence, we may reduce to the case where the first $k' < k$ iterates $f_a^i(x)$ lie outside $[1-a, a-1]$. Then the proposition holds for the iterates of $f_a^{k'+1}(x)$, since they behave like g_a. But $|Df_a| \geq 2a(a-1) \geq 2a_0(a_0-1)$ for the first k' iterates, which preserves the exponential estimates.

The proof for the case $g_a : x \longmapsto 1 - ax^2$ we adapt from Benedicks & Carleson [12], Lemma 1. (i) Let $\varphi : I \longrightarrow I$ be the homeomorphism $\varphi(\theta) = \sin(\frac{\pi}{2}\theta)$,[1] and write $\tilde{g}_a = \varphi^{-1} \circ g_a \circ \varphi$. Then, it is straightforward to compute that

$$D\tilde{g}_a(\theta) = 2\sqrt{1 - \frac{2-a}{2 - a\sin^2(\frac{\pi x}{2})}}.$$

Let $j \leq k-1$ denote the first return of x into the neighbourhood $[-1+2\delta^2, 1-2\delta^2]$. (If there is no such return, then one can take $j = k$ in the following reasoning.) Write $y_i = g_a^i(x)$. Since $|y_j| \geq \delta$ respectively $|y_j| \leq 1 - 2\delta^2$, we have

$$y_{j+1} = 1 - a(y_j)^2 \leq 1 - a\delta^2 \text{ respectively}$$
$$y_{j+1} \geq 1 - a(1 - a\delta^2)^2 = (1-a) + a\delta^2(2a - a^2\delta^2) \geq -1 + a\delta^2.$$

[1] Note that φ is a full conjugacy between $x \longmapsto 1 - 2x^2$ and the tent map $x \longmapsto 1 - 2|x|$.

By induction, we get $|y_i| \le 1 - a\delta^2$ for all $i = j, \dots, k$. For such i, we have

$$1 - \frac{1}{4}|D\tilde{g}_a(\varphi^{-1}(y_i))|^2 = \frac{2-a}{2-ay_i^2} \le \frac{2-a}{2-a(1-a\delta^2)^2} = \frac{1}{1+a^2\delta^2(\frac{2-a\delta}{2-a})}.$$

If δ is fixed, then the right hand side can be made arbitrarily small by choosing a_0 close enough to 2. (This step fails when tried directly for f_a instead of g_a.) Now write $g_a^k = \varphi \circ \tilde{g}_a^{k-j} \circ \varphi^{-1} \circ g_a^j$, then all together, the chain rule gives

$$\begin{aligned}
|Df_a^k(x)| &= |D\varphi(\varphi^{-1}(y_k))| \cdot \left| \prod_{i=j}^{k-1} D\tilde{g}_a(\varphi^{-1}(y_i)) \right| \cdot |D\varphi^{-1}(y_j)| \cdot |Dg_a^j(x)| \\
&= \sqrt{1-y_k^2} \cdot \left| \prod_{i=j}^{k-1} 2\sqrt{1 - \frac{2-a}{2-ay_i^2}} \right| \cdot \frac{1}{\sqrt{1-y_j^2}} \cdot \left| \prod_{i=0}^{j-1} 2ay_i \right| \\
&\ge \frac{\sqrt{1-y_k^2}}{\sqrt{1-y_j^2}} \cdot e^{\gamma_0(k-j)} \cdot (2a_0)^j (1-2\delta^2)^j.
\end{aligned}$$

Since $|y_k| \le 1 - a\delta^2$, we have $\sqrt{1-y_k^2} \ge \sqrt{2a\delta^2 - a^2\delta^4} \ge \delta\sqrt{2-\delta^2}$. This concludes part (i).

(iii) Suppose $e^{-\Delta} \le \delta$, then by the previous we may choose a_0 close enough to 2 to maintain the same exponent γ_0. Now, since $\delta < \frac{\sqrt{5}-1}{4}$ it is possible to choose a_0 sufficiently close to 2 so that necessarily $|y_j| \ge \delta$, otherwise y_j would not be the *first* return to $[-1+2\delta^2, 1-2\delta^2]$. Together with the assumption $|y_k| \le \delta$, it follows that $\sqrt{1-y_k^2}/\sqrt{1-y_j^2} \ge 1$.

(ii) Let $j \le k-1$ be the largest integer such that $y_j \in W$. Then $y_i \notin W$ for $i = j+1, \dots, k-1$, so $|Dg_a^{k-j-1}(y_{j+1})| \ge C_0 \cdot e^{\gamma_0(k-j-1)}$ by part (i). Also, $|Dg_a^j(x)| \ge e^{\gamma_0 j}$ by part (iii). Applying the chain rule to all this, we get

$$\begin{aligned}
|Dg_a^k(x)| &= |Dg_a^{k-j-1}(y_{j+1})| \cdot |Dg_a^j(x)| \cdot |Dg_a(y_j)| \\
&\ge C_0 \cdot e^{\gamma_0(k-j-1)} \cdot e^{\gamma_0 j} \cdot |2ay_j| \\
&\ge C_0 \cdot e^{\gamma_0 k} \cdot \inf_{0 \le i \le k-1} |y_i|.
\end{aligned}$$

This concludes (ii), and the proof of the proposition. ■

We shall now fix the following constants for the rest of the section.

- Fix the exponents $0 < \gamma < \frac{1}{40} \le \gamma_0 < \log(2)$.
- Set $\overline{\gamma} = \sup_{a,x} |Df_a(x)| = 4$. Then fix exponents $\alpha, \beta, \tau > 0$ with $\alpha < \beta \ll \gamma^2/(\gamma + \overline{\gamma})$ and $\tau < (\gamma_0 - \gamma - \alpha)/\gamma_0$.
- From Proposition 6.2, fix $K \in (0,1)$. As in the proposition, choose N_0 such that $\sum_{k=N_0}^{\infty} e^{-\gamma k} \le K$. It seems desirable to choose K close to 0, but at the cost of increasing N_0. Fix $N \ge \max\{N_0, \frac{1}{\alpha}, \frac{1}{\beta-\alpha}\}$.
- Fix the neighbourhood length $\delta < \frac{3}{40}$.

In contrast, the following variables appearing in propositions may change during the course of the section, and many definitions will implicitly depend on them.

– Let C_0, Δ and a_0 be such that all propositions established thus far (including the remark after Propositions 6.4) continue to hold. The constant C_0 is used in lower bounds, and it will decrease during the proof, so to maintain all inequalities. Other constants will usually be absorbed into it without mention. The same goes for the related constant C, which will increase from $C = \frac{1}{1-K}$ onward, and is used only in upper bounds. We shall always increase C or decrease C_0 to maintain $C_0 = 1/C$.

– Increasing Δ (which now already satisfies $U_\Delta \subseteq W_\delta$) will also maintain the truth of all propositions. Likewise, we increase $a_0 < 2$, but always in such a way that Proposition 6.4(iii) is maintained.

6.2. The concept of free returns. Fix a parameter value a for the moment. For all $n \geq 1$, we hope to obtain uniform exponential estimate for the derivative $\partial_x f_a^n(\xi_1) = \Pi_{i=1}^n -2a\xi_i$. This will clearly never happen if the critical point is periodic, that is, $\xi_\nu(a) = 0$ for some $\nu \geq 1$. For example, for the golden ratio $a = (1+\sqrt{5})/2$, the critical point of f_a has period two. Later on, we shall exclude such parameters. For now, we will partition the orbit $\xi_1, \xi_2, \ldots, \xi_n$, in order to appropriately apply chain rule to the specific pieces. The partition is as follows:

$$\begin{aligned}
&\xi_1, \ldots, \xi_{\nu_1}, && \text{(free orbit)}\\
&\xi_{\nu_1+1}, \ldots, \xi_{\nu_1+p_1}, && \text{(bound orbit)}\\
&\xi_{\nu_1+p_1+1}, \ldots, \xi_{\nu_2}, && \text{(free orbit)}\\
&\xi_{\nu_2+1}, \ldots, \xi_{\nu_2+p_2}, && \text{(bound orbit)}\\
&\xi_{\nu_2+p_2+1}, \ldots, \xi_{\nu_3}, && \text{(free orbit)}\\
&\quad\vdots\\
&\xi_{\nu_s+1}, \ldots, \xi_n && \text{(bound orbit) if } n \leq \nu_s + p_s\\
&\xi_{\nu_s+p_s+1}, \ldots, \xi_n, && \text{(free orbit) if } \nu_s + p_s < n \leq \nu_{s+1}.
\end{aligned}$$

The integers ν_i and p_i demarcate the *free* orbits and the *bound* orbits, and they are to be defined now.

Definition 6.6. Note again that the following terminologies implicitly depend on the neighbourhood $U = U_\Delta$, as well as on the fixed constant $\beta > 0$.

(i) Recall that the *first free return* (possibly infinity) is defined as

$$\nu_1(a) = \inf\{k > 0 : \xi_k(a) \in U\}.$$

(ii) If ν is a return, let r be the integer such that $\xi_\nu(a) \in I_r$. Define the corresponding *binding period* as the maximal integer $p = p(r, a)$ such that

$$\sup_{y \in U_r} |f_a^j(y) - f_a^j(0)| \leq e^{-\beta j} \qquad \text{for all } j = 0, \ldots, p. \tag{BC}$$

This binding condition we denote as BC. In particular, the condition 'binds' the orbit of $\xi_\nu(a)$ to the orbit of 0. Now, as mentioned it could be that $0 \in \xi_\nu(a)$. Because of this possibility we set $I_\infty = I_{\infty,0} = \{0\}$, then $r = \infty$ and also $p(\infty, a) = \infty$.

(iii) Inductively, suppose that ν_i is a free return, and let p_i be its corresponding binding period. The *next free return* $\nu_{i+1}(a)$ is the greatest integer ν (possibly infinity) such that $\xi_j(a) \notin U_\Delta$ for all $j = \nu_i + p_i + 1, \dots, \nu - 1$.

(iv) Suppose that s (possibly 0) is the number of all free returns $\nu_i(a) \le n$. For $i = 1, \dots, s-1$, define integers $q_i = q_i(n, a)$ so that $\nu_i + p_i + q_i = \nu_{i+1} - 1$. For $i = s$, define q_s as if to truncate the orbit at n:

$$q_s(n,a) = \begin{cases} n - (\nu_s + p_s) & \text{if } \nu_s + p_s < n \le \nu_{s+1}, \\ 0 & \text{if } n \le \nu_s + p_s. \end{cases}$$

Lastly, set $q_0(n, a) = \nu_1(a)$.

Let us elaborate on the above definition a little further in the following paragraph.

6.3. The conditions BA *and* FA. Suppose that ν is a return. Then the orbit of ξ_ν is bound to the orbit of $\xi_0 = 0$ for $p(r, a)$ amount of time, in the sense that $|\xi_{\nu+i} - \xi_i| \le e^{-\beta i}$ for $i \le p$. The idea here is that the first iterates of the point ξ_0 pick up an exponential derivative (by Proposition 6.4), and therefore so should the first p iterates of ξ_ν. This should compensate for the small derivative $Df_a(\xi_\nu)$. However, even with the condition $|\xi_{\nu+i} - \xi_i| \le e^{-\beta i}$, it may happen that $\xi_{\nu+i}$ nears 0 too closely. Therefore, we shall exclude some parameters to ensure that $\xi_{\nu+i}$ stays far enough away from 0. Specifically, we restrict to parameters satisfying the following *basic assumption*:

$$|\xi_k(a)| \ge 2 \cdot e^{-\alpha k} \qquad \text{for all } k = N, \dots, n. \tag{BA_n}$$

(The factor 2 will become clear later.) The choice $\alpha < \beta$ ensures that $\xi_{\nu+i}$ is closer to ξ_i than to 0. Note also that any $a \in [a_0, 2]$ automatically satisfies $\mathsf{BA}_{\nu_1 - 1}$ by Proposition 6.4(iii) and the choice of N.

The condition BA will imply that we have a loss of derivative at time n which no less than a factor $e^{-\alpha n}$. This loss will be compensated for by the free orbit, where $\xi_k \notin U_\Delta$ and so Proposition 6.5(iii) applies. In order to properly compensate, the free orbits need to be of sufficient length, and for this we need to exclude more parameters. To formalise this, define the integer $F_n(a) = \sum_{i=0}^{s} q_i(n, a)$, which equals the total time spent in free orbits. Then we restrict to parameters satisfying the following *freedom assumption*:

$$\frac{F_k(a)}{k} > 1 - \tau \qquad \text{for all } k = 1, \dots, n. \tag{FA_n}$$

As a side note, it is clear that the conditions BA_n and FA_n are always satisfied for $a = 2$ for all n. Let BA_n and FA_n denote the sets of values $a \in [a_0, 2]$ satisfying the corresponding conditions. Note that the set FA_n strongly depends on the neighbourhood U_Δ.

The ideas behind the conditions BA and FA will now be formalised by proving the following theorem.

Theorem 6.7. *For all Δ sufficiently large, there exists $a_0 < 2$, such that if $n \ge N$ and $a \in BA_n \cap FA_n$, then*

$$|Df_a^k(\xi_1)| \ge e^{\gamma k} \qquad \textit{for all } k = 1, \dots, n. \tag{EX_n}$$

The conclusion of this theorem is denoted as statement EX_n, and we denote the set of corresponding parameters by $EX_n = \{a \in [a_0, 2] : \mathsf{EX}_n \text{ holds for } a\}$. Each EX_n is equal to a finite union of compact intervals, since it is a finite intersection of pre-images of half-lines under the polynomial maps $a \longmapsto Df_a^k(\xi_1)$.

We will now prove Theorem 6.7 by induction on n. By the remark after Proposition 6.4 (or equally well, by Proposition 6.5(i)), the base case $n = N$ is true. Now assume that $a \in BA_n \cap FA_n \cap EX_{n-1}$, then we show that $a \in EX_n$. For this we first show that the binding period following a free return is of sufficient length to compensate the small constant C_0 arising from Proposition 6.5.

Lemma 6.8. *There exists $C_0 > 0$ such that for each Δ sufficiently large, there exists $a_0 < 2$, such that if $n \geq N$ and $a \in BA_n \cap EX_{n-1}$, the following holds. Suppose $\nu \leq n$ is a return into $U_{\Delta-1}$, and let $p = p(r, a)$ be the binding period with $r \geq \Delta - 1$. Then*

(i) $p \leq 3r/\gamma \leq 3\alpha\nu/\gamma \ll \nu$,

(ii) *for all $x \in U_r$,*

$$C_0 \leq \frac{|Df_a^j(f_a(x))|}{|Df_a^j(f_a(0))|} \leq \frac{1}{C_0} \quad \text{for } j = 1, \ldots, p,$$

(iii) $p \geq C_0 \cdot r$, *and* $|Df_a^{p+1}(x)| \geq e^{\gamma p/4}$ *for all* $x \in I_r$.

Proof. Using the formula $Df_a^k(x) = \prod_{i=0}^{k-1} -2af_a^i(x)$, consider for $j \leq \min\{p, n\}$

$$\frac{|Df_a^j(f_a(x))|}{|Df_a^j(f_a(0))|} = \prod_{i=1}^{j} \frac{|f_a^i(x)|}{|f_a^i(0)|}. \tag{6.4}$$

For $i = 1, \ldots, N$, it holds that $|f_a^i(0)|, |f_a^i(x)| \geq \frac{1}{2}$ by Proposition 6.4(i). For $i = N, \ldots, \min\{p, n\}$ the conditions BC and BA hold with $\alpha < \beta$. Together with the general inequality $\log y \leq y - 1$, this shows the two inequalities

$$\log \prod_{i=N}^{j} \frac{|f_a^i(x)|}{|f_a^i(0)|} \leq \sum_{i=N}^{\min\{p,n\}} \frac{|f_a^i(x) - f_a^i(0)|}{|f_a^i(0)|} \leq \sum_{i=N}^{\infty} e^{(\alpha-\beta)i} \leq C,$$

$$\log \prod_{i=N}^{j} \frac{|f_a^i(0)|}{|f_a^i(x)|} \leq \sum_{i=N}^{\min\{p,n\}} \frac{|f_a^i(x) - f_a^i(0)|}{|f_a^i(0)| - |f_a^i(x) - f_a^i(0)|} \leq \sum_{i=N}^{\infty} \frac{1}{e^{(\beta-\alpha)i} - 1} \leq C.$$

All these facts show that (6.4) is bounded from below and above for $j \leq \min\{p, n\}$. We need to show $p \leq n$. To do this, we start by considering

$$\begin{aligned} \frac{f_a^j(f_a(x)) - f_a^j(f_a(0))}{f_a(x) - f_a(0)} \frac{1}{Df_a^j(f_a(0))} &= \prod_{i=1}^{j} \frac{f_a(f_a^i(x)) - f_a(f_a^i(0))}{f_a^i(x) - f_a^i(0)} \frac{1}{2af_a^i(0)} \\ &= \prod_{i=1}^{j} \frac{f_a^i(x) + f_a^i(0)}{2f_a^i(0)}. \end{aligned} \tag{6.5}$$

Let $y_i = f_a^i(x)/f_a^i(0)$, then in fact $y_i > 0$ for $i \leq \min\{p, n\}$. By taking logarithms, the products $\prod_{i=N}^{j}(y_i + 1)/2$ and $\prod_{i=N}^{j} 2/(y_i + 1)$ are bounded above since the

sum $\sum_{i=N}^{j} y_i - 1$ is as shown previously. Therefore, (6.5) is also bounded from below and above by positive constants. Now suppose $x \in I_r$. The lower bound on (6.5) implies that if $a \in EX_{n-1}$ and $j \leq \min(p, n-1)$, then

$$C_0 \cdot e^{\gamma j} \cdot ae^{-2r-2} \leq |f_a^{j+1}(x) - f_a^{j+1}(0)| \leq 2.$$

In particular, it follows that $\min(p, n-1) \leq 3r/\gamma$ provided that Δ is sufficiently large. Note that $f_a^{\nu}(0) \in I_r$ and $|f_a^{\nu}(0)| \geq e^{-\alpha\nu}$ imply $r \leq \alpha\nu$, so it follows that $p \leq 3r/\gamma \leq 3\alpha\nu/\gamma \ll \nu$. This proves part (i) and (ii). The upper bound on (6.5) together with the definition of p implies the inequalities

$$e^{-\beta(p+1)} < |f_a^{p+1}(x) - f_a^{p+1}(0)| \leq C \cdot |Df_a^p(f_a(0))| \cdot ae^{-2r} \leq C \cdot e^{\overline{\gamma}p} \cdot e^{-2r}.$$

Since $\beta \ll 1$, it follows that $p \geq C_0 \cdot r$ for some $C_0 > 0$ sufficiently small. From part (ii) and the previous inequality, we also get

$$\begin{aligned} |Df_a^{p+1}(x)| = |2ax| \cdot |Df_a^p(f_a(x))| &\geq C_0 \cdot e^{-r} \cdot |Df_a^p(f_a(0))| \\ &\geq C_0 \cdot \sqrt{\frac{e^{-\beta p}}{Df_a^p(f_a(0))}} \cdot |Df_a^p(f_a(0))| \\ &\geq C_0 \cdot e^{(\gamma-\beta)p/2}. \end{aligned}$$

The last expression is at least as big as $e^{\gamma p/4}$ provided that $p \geq C_0 \cdot \Delta$ is sufficiently large, proving (iii). ■

Proof of Theorem 6.7. If $n \leq \nu_1(a)$, then the conclusion follows from Proposition 6.5(i) and the choice of N. Otherwise, we can apply the chain rule to partitioned orbit described earlier:

$$|Df_a^n(\xi_1)| = |Df_a^{\nu_1-1}(\xi_1)| \cdot \left| \prod_{i=1}^{s-2} Df_a^{\nu_{i+1}-\nu_i}(\xi_{\nu_i}) \right| \cdot |Df_a^{n+1-\nu_s}(\xi_{\nu_s})|. \tag{6.6}$$

For the first factor in (6.6) we have $|Df_a^{\nu_1-1}(\xi_1)| \geq e^{\gamma(q_0-1)}$ because $a \in EX_{n-1}$. For the second factor, note that $\xi_j \notin U_\Delta$ for $j = \nu_i + p_i + 1, \ldots, \nu_{i+1} - 1$ and $\xi_{\nu_{i+1}} \in U_\Delta$ by definition of ν_{i+1}, so by Proposition 6.5(iii) and the previous lemma, we have

$$|Df_a^{\nu_{i+1}-\nu_i}(\xi_{\nu_i})| = |Df_a^{q_i}(\xi_{\nu_i+p_i+1})| \cdot |Df_a^{p_i+1}(\xi_{\nu_i})| \geq e^{\gamma_0 q_i} \cdot e^{\gamma p_i/4}.$$

For the third factor in (6.6) we have two cases. *Case 1:* $n > \nu_s + p_s$. Recall that for $j \leq n$ we assume that $|\xi_j| \geq e^{-\alpha j}$, and again it holds that $\xi_j \notin U_\Delta$ for $j = \nu_s + p_s + 1, \ldots, n$, so Proposition 6.5(ii) gives

$$|Df_a^{n+1-\nu_s}(\xi_{\nu_s})| \geq C_0 \cdot e^{\gamma_0 q_s} \cdot \inf_{\nu_s+p_s \leq j \leq n} |\xi_j| \geq C_0 \cdot e^{\gamma_0 q_s} \cdot e^{-\alpha n}.$$

Case 2: $n \leq \nu_s + p_s$. Using part (ii) of the previous lemma, we get

$$\begin{aligned} |Df_a^{n+1-\nu_s}(\xi_{\nu_s})| &= |Df_a^{n-\nu_s}(\xi_{\nu_s+1})| \cdot |Df_a(\xi_{\nu_s})| \\ &\geq C_0 \cdot |Df_a^{n-\nu_s}(\xi_1)| \cdot 2a|\xi_{\nu_s}| \\ &\geq C_0 \cdot e^{\gamma(n-\nu_s)} \cdot e^{-\alpha n}. \end{aligned}$$

In both cases, we get in total

$$|Df_a^n(\xi_1)| \geq C_0 \cdot e^{\gamma_0 F_n} \cdot e^{\gamma(n-F_n)/4} \cdot e^{-\alpha n}.$$

Since $p_i \geq C_0 \cdot \Delta$ by the previous lemma, it holds that $n - F_n \geq C_0 \cdot s \cdot \Delta$. Therefore, $C_0 \cdot e^{\gamma(n-F_n)/4} \geq 1$ for Δ sufficiently large. Using $a \in FA_n$, we are reduced to

$$|Df_a^n(\xi_1)| \geq e^{\gamma_0(1-\tau)n} \cdot e^{-\alpha n} \geq e^{\gamma n}.$$

The last estimate follows from the choice $\tau < (\gamma_0 - \gamma - \alpha)/\gamma_0$. ■

6.4. Partitioning the set of parameters. We have now established exponential growth of Df_a^n for the parameters $a \in BA_n \cap FA_n$. The aim is now to show that the set of such parameters has positive measure. For this it is necessary to split up the set of parameters into small intervals $\omega \subseteq [0, 2]$ and analyse the length of each interval. We start by stating a lemma on the length of $|\xi_i(\omega)|$ compared to $|\xi_n(\omega)|$ when $i \ll n$.

Lemma 6.9. *Let $n \geq 1$, and suppose that $\omega \subseteq EX_{n-1}$ is an interval. Then the map $\xi_n : \omega \longrightarrow I$ is a diffeomorphism onto its image, and $|\xi_n(\omega)| \geq C_0 \cdot e^{\gamma n} \cdot |\omega|$. In general, if $i \leq 3\alpha n/\gamma$ and n is sufficiently large, then $|\xi_n(\omega)| \geq |\xi_i(\omega)|$.*

Proof. The proof that $\xi_n : \omega \longrightarrow I$ is a diffeomorphism onto its image is the same as for Proposition 6.4(ii). Using this, suppose that ω has endpoints $a < b$, then the mean value theorem gives $c, d \in \omega$ such that

$$\frac{|\xi_n(\omega)|}{|\xi_i(\omega)|} = \frac{|\xi_n(a) - \xi_n(b)|}{|a-b|} \cdot \frac{|a-b|}{|\xi_i(a) - \xi_i(b)|} = \frac{|\partial_a f_c^n(\xi_0)|}{|\partial_a f_d^i(\xi_0)|}.$$

By Proposition 6.2, the right hand side is at least $C_0 \cdot \frac{e^{\gamma n}}{4^i} \geq C_0 \cdot e^{\gamma n - \frac{3\alpha \log(4)}{\gamma} n}$. Since $\alpha < \gamma^2/5$, the latter is at least 1 provided that n is sufficiently large. ■

Next, we are going to partition the parameter intervals ω. To do this, we first generalise the definition of returns ν_i and binding periods p_i from dependence on a single parameter a to dependence on an entire interval ω. More precisely, the following definition reduces to Definition 6.6 when $\omega = \{a\}$.

Definition 6.10. Let $\omega \subseteq [0, 2]$ be a parameter interval. An integer $\nu \leq n$ is called a *return* for ω if $\xi_\nu(\omega) \cap U_\Delta \neq \varnothing$. Define the *first free return* of ω as

$$\nu_1(\omega) = \inf\{k > 0 : \xi_k(\omega) \cap U_\Delta \neq \varnothing\}.$$

Suppose ν is a return, and let r be the maximal integer such that $\xi_\nu(\omega) \cap I_r \neq \varnothing$. Set $p(r, \omega) = \min_{a \in \omega} p(r, a)$, where $p(r, a)$ is the binding period as defined by condition BC. If $\nu_i(\omega)$ is a free return with binding period $p_i = p_i(r, \omega)$, the *next free return* ν_{i+1} is the greatest integer ν (possibly infinity) such that $\xi_j(\omega) \cap U_\Delta = \varnothing$ for all $j = \nu_i(\omega) + p_i(r, \omega) + 1, \ldots, \nu - 1$.

For each $n \geq N$, we now construct a partition $\mathscr{E}_n$ of the set EX_{n-1}. The following notation will be helpful with formulations. Suppose $\mathscr{E}$ is any collection

of parameter intervals, and J is any subset of parameters. Then define the notation

$$\mathscr{E}|J = \{\omega \cap \omega' : \omega \in \mathscr{E}, \text{ and } \omega' \text{ is a connected component of } J\}.$$

In this way, $\mathscr{E}|J$ is a new a collection of intervals, which arises from $\mathscr{E}$ restricted to J.

Now we inductively construct $\mathscr{E}_n$: set $\mathscr{E}_N = \{[a_0, 2]\}$, and suppose that $\mathscr{E}_{n-1}$ is defined. To define $\mathscr{E}_n$, consider $\omega \in \mathscr{E}_{n-1}|EX_{n-1}$. If n *is not* a free return of ω, then we simply let $\omega \in \mathscr{E}_n$. If n *is* a free return of ω, then consider the interval $\xi_n(\omega)$ which possibly contains 0. Write a disjoint union

$$\xi_n(\omega) = \Omega \cup \bigcup_i I_{r_i,\ell_i},$$

where $\bigcup_i I_{r_i,\ell_i}$ (possibly empty) equals a single interval inside U_Δ, and Ω has two disjoint components either of which is equal to one of the following:

- a component of $\xi_n(\omega) \setminus U_\Delta$ which fully contains $I_{\Delta-1,1}$ or $I_{\Delta-1,-1}$;
- an interval $I_{r,\ell}$ with $r \geq \Delta$ plus possibly smaller pieces of the two neighbouring intervals $I_{r',\ell'}$;
- a smaller piece of some $I_{r,\ell}$ with $r \geq \Delta - 1$, provided that $\bigcup_i I_{r_i,\ell_i}$ is empty and neither of the above is possible.

Now, consider ξ_n as a diffeomorphism $\xi_n : \omega \longrightarrow I$ as in Lemma 6.9. Then, the two components of Ω together with the intervals I_{r_i,ℓ_i} correspond exactly to subintervals $\omega_{r_i,\ell_i} \subseteq \omega$ by taking pre-images under ξ_n. Each of these subintervals ω_{r_i,ℓ_i} we put in $\mathscr{E}_n$. This completes the definition of $\mathscr{E}_n$.

Let us state some immediate consequences of this construction. Firstly, the partition $\mathscr{E}_n$ indirectly defines a partition of BA_n. Namely, define

$$\mathscr{B}_n = \{\omega \in \mathscr{E}_n : \omega \cap BA_n \neq \varnothing\}.$$

The following lemma shows that $\mathscr{B}_n$ is a finite partition, whereas $\mathscr{E}_n$ is at most countable by the above construction.

Lemma 6.11. *For Δ sufficiently large, there exists $a_0 < 2$ such that $n \geq N$ and $\omega \in \mathscr{E}_n$ imply that*

(i) *if n is a free return of ω, then $\xi_n(\omega) \subseteq U_{\Delta-1}$ and $|\xi_n(\omega)| \leq 4 \cdot e^{-r}/r^2$;*

(ii) *if $a \in \omega$ and there exists $b \in \omega \cap BA_n$, then*

$$|\xi_k(a)| \geq e^{-\alpha k} \qquad \text{for } k = N, \ldots, n. \tag{BA'_n}$$

Proof. (i) Let $r \leq \Delta$ be the maximal integer with $\xi_\nu(\omega) \cap I_r \neq \varnothing$. Then by definition $|\xi_\nu(\omega)| \leq |I_{r,r^2-1}| + |I_{r-1,1}| + |I_{r-1,2}|$ and a straightforward estimation shows that the latter is at most $4 \cdot e^{-r}/r^2$

(ii) Suppose first that n is a free return of ω. Say that $\xi_n(b) \in I_{r,\ell}$ with $\ell > 0$ (the case $\ell < 0$ is similar). Using part (i) and the fact $|\xi_n(b)| \geq 2 \cdot e^{-\alpha n}$, a straightforward but tedious estimation shows that

$$\begin{aligned} |\xi_n(a)| \quad \geq \quad |\xi_n(b)| - |\xi_n(a) - \xi_n(b)| \quad &\geq \quad (\sup I_{r,\ell}) - 4 \cdot e^{-r}/r^2 \\ &\geq \quad \frac{1}{2} \cdot \sup I_{r,\ell} \quad \geq \quad e^{-\alpha n}. \end{aligned}$$

If $n > \nu_1$ is not a return, then by the previous $|\xi_n(a)| \geq e^{-\Delta} \geq e^{-\alpha\nu_1} \geq e^{-\alpha n}$. Lastly, suppose n is a bound return, that is, $\nu < n \leq \nu + p$ for some free return ν. Since $\xi_\nu(b) \in U_{\Delta-1}$, we have $n - \nu \leq 3\alpha\nu/\gamma$ by Lemma 6.8. Then, by the second part of Lemma 6.9, we get

$$\begin{aligned} |\xi_n(a)| &\geq |\xi_{n-\nu}(b)| - |\xi_{n-\nu}(b) - \xi_{n-\nu}(a)| - |\xi_{n-\nu}(a) - \xi_n(a)| \\ &\geq 2 \cdot e^{-\alpha(n-\nu)} - 4 \cdot \frac{e^{-r}}{r^2} - e^{-\beta(n-\nu)} \quad \geq \quad e^{-\alpha n}. \end{aligned}$$

This covers all cases for n, finishing the proof of the lemma. ■

6.5. Exclusion of parameters. Let BA'_n denote the set of parameters partitioned by $\mathscr{B}_n$. Part (ii) of Lemma 6.12 implies that all estimates in both Lemma 6.8 and Theorem 6.7 remain true when assuming $a \in BA'_n$ instead of $a \in BA_n$. Now define E as the following monotone decreasing intersection:

$$E = \bigcap_{n \geq 1} BA'_n \cap FA_n.$$

Let us explain the strategy for proving that E has positive measure. If ω is an interval in $\mathscr{B}_{n-1}|EX_{n-1}$, then by Lemma 6.11, its subintervals $\tilde{\omega} \in \mathscr{E}_n$ which do *not* intersect BA_n are of the form $\tilde{\omega} = \omega_{r_i,\ell_i}$ with $r_i > \alpha n$. As such, we formulate the following.

Proposition 6.12. *There exists a constant $C_0 > 0$ such that if Δ is sufficiently large, there exists $a_0 < 2$ such that the following holds. If $n \geq 1$ and $\omega \in \mathscr{B}_{n-1}|EX_{n-1}$, then*

$$\frac{\left|\omega \setminus \bigcup_{r_i > \alpha n} \omega_{r_i,\ell_i}\right|}{|\omega|} \geq 1 - e^{-C_0 \alpha n}.$$

We shall prove this Lemma at the very end of this chapter. For now, we see that Proposition 6.12 implies that

$$\sum_{\omega \in \mathscr{B}_n} |\omega| \quad \geq \quad (1 - e^{-C_0\alpha n}) \cdot \left(\sum_{\omega \in \mathscr{B}_{n-1}|EX_{n-1}} |\omega| \right). \tag{6.7}$$

In Proposition 6.12 the set of points where BA'_n fails is excluded. A similar statement holds true when excluding the points where FA fails. If $\mathscr{P}_n$ denotes the connected components of $FA_n \cap (\mathscr{B}_{n-1}|EX_{n-1})$, of which there are finitely many, then

$$\sum_{\omega \in \mathscr{P}_n} |\omega| \quad \geq \quad (1 - e^{-\gamma\tau n/2}) \cdot \left(\sum_{\omega \in \mathscr{B}_{n-1}|EX_{n-1}} |\omega| \right). \tag{6.8}$$

We will not prove this last inequality; it is proved by lemmas V.6.6–V.6.9 in De Melo & Van Strien [8], using the concept of *essential* returns. Since $BA'_n \cap FA_n \subseteq EX_n$, taking the previous two inequalities together implies that

$$\operatorname{meas}(E) = \lim_{n \to \infty} \operatorname{meas}(BA'_n \cap FA_n) \geq (2 - a_0) \cdot \prod_{k=1}^{\infty} 1 - e^{-C_0 k}.$$

6.6. Uniformness of parameter derivatives. To prove the two inequalities (6.7) and (6.8) on excluded parameters, results are needed on the uniformity of parameter derivatives over the small intervals in $\mathscr{E}_n^\circ$. Here, uniformity is characterised using the notion of *distortion*; we refer to Appendix B for a discussion on this topic. In Lemma 6.8(ii) we have seen distortion already: for the correct parameter values a and for $r \geq \Delta - 1$, it holds that f_a^{j-1} has bounded distortion on $f_a(U_r)$ for $j = 1, \ldots, p(r,a)+1$. For these j, and any subinterval $J \subseteq U_r$, it follows that

$$|Df_a^{j-1}(\xi_1)| \leq C \cdot \inf_{x \in J} |Df_a^{j-1}(f_a(x))| \leq C \cdot \frac{|f_a^j(J)|}{|f_a(J)|} \leq C \cdot \frac{|f_a^j(J)|}{e^{-2r}}. \tag{6.9}$$

This will be used in the following lemma. Recall that the *Hausdorff-distance* between sets A and B satisfies $d_{\mathrm{H}}(A,B) \leq \varepsilon$ if for all $x \in A$, there exists $y \in B$ with $d(x,y) \leq \varepsilon$ and vice versa. We shall freely use the inequality $|\operatorname{diam}(A) - \operatorname{diam}(B)| \leq 2 \cdot d_{\mathrm{H}}(A,B)$ without mention, since it is easy to prove from the previous characterisation of d_{H}.

Lemma 6.13. *Fix $\varepsilon \in (0, \frac{1}{2}]$ small. For Δ sufficiently large, there exists $a_0 < 2$ such that the following holds. Suppose $n \geq N$, and suppose $\omega \in \mathscr{B}_{n-1}$ has a free return at $\nu \leq n-1$. Then for all $a, b \in \omega$, all subintervals $J \subseteq U_{r-1}$, and all $j = 1, \ldots, p(r,\omega)+1$ we have*

$$d_{\mathrm{H}}(f_a^j(J), f_b^j(J)) \leq \varepsilon \cdot |f_a^j(J)|. \tag{6.10}$$

In particular, for any subinterval $\tilde{\omega} \subseteq \omega$, we have

$$d_{\mathrm{H}}(f_a^j(\xi_\nu(\tilde{\omega})), \xi_{\nu+j}(\tilde{\omega})) \leq \varepsilon \cdot |f_a^j(\xi_\nu(\tilde{\omega}))|. \tag{6.11}$$

Proof. For $y \in J$, write $f_a^j(y) - f_b^j(y) = \partial_a f_c^j(y)(a-b)$ for some $c \in [a,b]$. By a general inequality for partial derivatives (see formula (B.1) in Appendix B), we have

$$|\partial_a f_a^j(y)| \leq |Df_a^{j-2}(f_a(y))| \cdot \left(4 + \sum_{i=0}^{j-2} \frac{1}{|Df_a^i(f_a(y))|}\right).$$

First observing that the denominator on the right hand side is exponentially increasing by Lemma 6.8(ii), and then applying inequality (6.9), we have

$$|\partial_a f_a^j(y)| \leq C \cdot |Df_a^{j-2}(\xi_1)| \leq C \cdot |Df_a^{j-1}(\xi_1)| \leq C \cdot \frac{|f_a^j(J)|}{e^{-2r}}.$$

Using the bound on $|\xi_\nu(\omega)|$ and subsequently Lemma 6.9, we obtain

$$\begin{aligned} |f_a^j(y) - f_b^j(y)| \leq |\partial_a f_c^j(y)| \cdot |a-b| &\leq C \cdot \frac{|f_c^j(J)|}{e^{-2r}} \cdot |\omega| \\ &\leq C \cdot |f_c^j(J)| \cdot \frac{e^{-r}/r^2}{e^{-2r}} \cdot \frac{|\omega|}{|\xi_\nu(\omega)|} \\ &\leq C \cdot |f_c^j(J)| \cdot e^{-\gamma\nu+r}/r^2. \end{aligned}$$

If $\omega \in BA'_{n-1}$, then $r < \alpha\nu$, so for a_0 sufficiently close to 2,

$$d_{\mathrm{H}}(f_a^j(J), f_b^j(J)) \leq \frac{\varepsilon}{2} \cdot |f_c^j(J)|.$$

Now let $d \in [a,b]$ be such that $|f_d^j(J)| = \max_{c' \in [a,b]} |f_{c'}^j(J)|$. Then by the previous,

$$d_{\mathrm{H}}(f_a^j(J), f_d^j(J)) \leq \frac{\varepsilon}{2} \cdot |f_d^j(J)|.$$

Since $\varepsilon \leq 1/2$, this implies in general that $|f_d^j(J)| \leq 2 \cdot |f_a^j(J)|$ which finishes the proof. The second inequality follows since the first holds for all $b \in \omega$. ■

Corollary 6.14. *Under the premises of the previous proposition, the results from Lemma 6.8 hold for $a \in \omega$ when $p(r,a)$ is replaced by $p(r,\omega)$.*

Proof. Take $b \in \omega$ so that $p(r,b) = p(r,\omega)$, and let ε be sufficiently small. Inserting the following estimates are into the proof of Lemma 6.8 gives the proof of point (iii) of the lemma:

$$|f_a^{p(r,\omega)+1}(U_r)| \geq (1-\varepsilon) \cdot |f_b^{p(r,b)+1}(U_r)| \geq (1-\varepsilon) \cdot e^{-\beta p(r,\omega)}.$$

Points (i) and (ii) of the lemma hold trivially. ■

We now come to showing that the parameter derivative of f_a^k on the small intervals ω is very uniform, in a sense that is described by the following main proposition.

Lemma 6.15. *There exists $C > 0$ such that if Δ is sufficiently large, there exists $\varepsilon > 0$ such that the following holds. Suppose that $\omega \in \mathscr{B}_{n-1}|EX_{n-1}$ where n is a free return of ω, and suppose that $\xi_n(\omega) \subseteq U_{\Delta/2}$. Then for all $a, b \in \omega$ we have*

$$\frac{|\partial_x f_a^k(\xi_1)|}{|\partial_x f_b^k(\xi_1)|} \leq C \quad \text{for } k = 0, \ldots, n-1, \tag{6.12}$$

$$\frac{|\partial_a f_a^k(\xi_0)|}{|\partial_a f_b^k(\xi_0)|} \leq C \quad \text{for } k = 0, \ldots, n.$$

The second inequality follows directly from the first inequality by Proposition 6.2. To prove the first inequality, we need another lemma. For the proof of the lemma, we need the following small construction. Suppose as usual that $\omega \subseteq EX_{n-1}$, and $j < k \leq n$. If $a, b \in \omega$, then as in the proof of Lemma 6.9, we have

$$|f_a^{k-j}(\xi_j(b)) - f_b^{k-j}(\xi_j(b))| \leq C \cdot e^{\overline{\gamma}(k-j)} \cdot e^{-\gamma j} \cdot |\xi_j(\omega)|. \tag{6.13}$$

(Alternatively, inequality (B.1) can be used to help show this.) We will need that the right hand side of this inequality is small, which is certainly not the case when $k - j \gg j$. But, when $k - j \leq \gamma j/(\gamma + \overline{\gamma})$, then by the choice of β we have $e^{\overline{\gamma}(k-j)} \cdot e^{-\gamma j} \leq e^{-\beta j}$.

With this in mind, we make a one-off partition of the orbit ξ_i by choosing integers $\nu + p + 1 = k_0 \leq k_1 \leq \cdots \leq k_u \leq \nu'$, where $\nu < \nu'$ are consecutive free returns of ω, and p is the binding period of ν. We do this as follows.

Step 1. Set $k_0 = \nu + p + 1$.

Step $i+1$. Suppose that k_i is defined. If $\xi_{k_i}(\omega)$ contains a component of $\{x : \delta \le |x| < 2\delta\}$, then $i = u$. If not then consider the section of integers $S_i = \{m : k_i < m \le k_i + \gamma k_i/(\gamma + \overline{\gamma})\}$, and do one of the following.

- If $\xi_m(\omega) \cap W_\delta = \varnothing$ for all $m \in S_i$, set $k_{i+1} = \max S_i$.
- If not, then set $k_{i+1} = \max\{m \in S_i : \xi_m(\omega) \cap W_\delta \neq \varnothing\}$.

In this way, it holds that $k_{i+1} - k_i \le \gamma k_i/(\gamma + \overline{\gamma})$ for $i = 0, \dots, u$. Moreover, by the definition of k_u and since $\xi_{\nu'}(\tilde{\omega}) \cap U \neq \varnothing$, it holds that $\nu' - k_u$ is bounded above by the same positive integer independent of the choice of a_0.

Lemma 6.16. *There exists a constant $C_0 > 0$ such that if Δ is sufficiently large, there exists $a_0 < 2$, such that if $n \ge N$ and $\omega \in \mathscr{B}_{n-1}|EX_{n-1}$, the following holds. Let $p = p(r, \omega)$ be the binding period of a free return ν, and let $\nu' \le n$ be the next free return. For any subinterval $\tilde{\omega} \subseteq \omega$, the length $|\xi_j(\tilde{\omega})|$ for $\nu < j \le \nu'$ can be estimated as follows.*

(i) *For $j = 1, \dots, p+1$,*

$$|\xi_{\nu+j}(\tilde{\omega})| \ge C_0 \cdot e^{\gamma j} \cdot |\xi_{\nu+1}(\tilde{\omega})|,$$
$$|\xi_{\nu+p+1}(\tilde{\omega})| \ge e^{\gamma p/4} \cdot |\xi_{\nu+1}(\tilde{\omega})|.$$

(ii) *For $j = \nu + p + 1, \dots, \nu'$,*

$$|\xi_{\nu'}(\tilde{\omega})| \ge C_0 \cdot e^{\gamma(\nu' - j)} \cdot |\xi_j(\tilde{\omega})|,$$
$$|\xi_{\nu'}(\tilde{\omega})| \ge 2 \cdot |\xi_\nu(\tilde{\omega})|.$$

Proof. (i) Suppose first that $1 \le j \le p+1$ and $a \in \omega$. First applying inequality (6.11), and then inequality (6.9), we have

$$\begin{aligned} |\xi_{\nu+j}(\tilde{\omega})| \ge C_0 \cdot |f_a^j(\xi_\nu(\tilde{\omega}))| &\ge C_0 \cdot |Df_a^{j-1}(\xi_1)| \cdot |f_a(\xi_\nu(\tilde{\omega}))| \\ &\ge C_0 \cdot e^{\gamma(j-1)} \cdot |f_a(\xi_\nu(\tilde{\omega}))|. \end{aligned}$$

Since a is arbitrary, the first inequality follows. By the same line of reasoning, but noting that inequality (6.9) still holds if the left hand side is replaced by $Df_a^{p+1}(x) = Df_a^p(f(x)) \cdot Df_a(x)$, and then using Corollary 6.14, we get $|\xi_{\nu+p+1}(\tilde{\omega})| \ge e^{\gamma p/4} \cdot |\xi_\nu(\tilde{\omega})|$. (ii) Suppose $\nu + p + 1 \le j < k \le \nu'$, and take $a < b$ as the endpoints of $\tilde{\omega}$. By the mean value theorem and (6.13), we have

$$\begin{aligned} |\xi_k(\tilde{\omega})| &\ge |f_a^{k-j}(\xi_j(a)) - f_a^{k-j}(\xi_j(b))| - |f_a^{k-j}(\xi_j(b)) - f_b^{k-j}(\xi_j(b))| \\ &\ge (|Df_a^{k-j}(y_j)| - C \cdot e^{\overline{\gamma}(k-j)} \cdot e^{-\gamma j}) \cdot |\xi_j(\tilde{\omega})|, \end{aligned}$$

for some $y_j \in \xi_j(\tilde{\omega})$. By (6.13), it follows that if a_0 is sufficiently close to 2 and $k - j \le \gamma j/(\gamma + \overline{\gamma})$, then

$$d_{\mathrm{H}}(f_a^{k-j}(\xi_j(\tilde{\omega})), \xi_k(\tilde{\omega})) \le e^{-\beta j} \cdot |\xi_j(\tilde{\omega})|. \tag{6.14}$$

With these observations, we distinguish three cases for the value of the index $0 \le i < u$.

Case 1: $\xi_{k_{i+1}}(\tilde{\omega}) \cap W_\delta \neq \varnothing$ but $\xi_{k_{i+1}}(\tilde{\omega})$ does not contain a component of $\{x : \delta \leq |x| < 2\delta\}$. By inequality (6.14), it follows that $f_a^{k_{i+1}-k_i}(\xi_{k_i}(\tilde{\omega})) \subseteq (-3\delta, 3\delta)$. Since it holds that $\xi_m(\tilde{\omega}) \cap U_\Delta = \varnothing$ for $k_i \leq m < k_{i+1}$, inequality (6.14) also implies that $f_a^{m-k_i}(\xi_{k_i}(\tilde{\omega})) \cap U_{\Delta+1} = \varnothing$, provided that a_0 is sufficiently close to 2. By Proposition 6.5(iii), this implies that $|Df_a^{k_{i+1}-k_i}(y_{k_i})| \geq e^{\gamma_0(k_{i+1}-k_i)}$.

Case 2: $\xi_{k_{i+1}}(\tilde{\omega}) \cap W_\delta \neq \varnothing$ and $\xi_{k_{i+1}}(\tilde{\omega})$ does contain a component of $\{x : \delta \leq |x| < 2\delta\}$. Then $i+1 = u$, and $\nu' - k_u$ is universally bounded from above. Therefore, Proposition 6.5(ii) implies that $|Df_a^{k_{i+1}-k_i}(y_{k_i})| \geq C_0 \cdot e^{\gamma_0(k_{i+1}-k_i)}$.

Case 3: $\xi_{k_{i+1}}(\tilde{\omega}) \cap W_\delta = \varnothing$. In this case, Proposition 6.5(i) immediately implies that $|Df_a^{k_{i+1}-k_i}(y_{k_i})| \geq C_0 \cdot e^{\gamma_0(k_{i+1}-k_i)}$.

To finalise, note that each k_{i+1} may be chosen greater than $k_i \cdot (1 + \frac{1}{2}\gamma/(\gamma + \overline{\gamma}))$. Thus, by choosing Δ large enough, the three cases together yield

$$\begin{aligned}
|\xi_{\nu'}(\tilde{\omega})| &\geq \Big(\prod_{k_i \geq j} |Df_a^{k_{i+1}-k_i}(f_a^{k_i}(y_j))| - C \cdot e^{\overline{\gamma}(k_{i+1}-k_i)} \cdot e^{-\gamma k_i}\Big) \cdot |\xi_j(\tilde{\omega})| \\
&\geq \Big(\prod_{k_i \geq j} C_0 \cdot e^{\gamma_0(k_{i+1}-k_i)} - e^{-\beta(k_{i+1}-k_i)} \cdot |\xi_j(\tilde{\omega})| \\
&\geq e^{\gamma(\nu'-j)} \cdot |\xi_j(\tilde{\omega})|.
\end{aligned}$$

The inequality $|\xi_{\nu'}(\tilde{\omega})| \geq 2|\xi_\nu(\tilde{\omega})|$ follows from the previous inequality, since $\nu' - \nu$ is arbitrarily large for Δ sufficiently large. ■

Proof of inequality (6.12). We need to estimate

$$\frac{|Df_a^k(f_a(0))|}{|Df_b^k(0)|} = \prod_{i=1}^{k} \frac{|f_a^i(0)|}{|f_b^i(0)|}. \tag{6.15}$$

Let $k_0 \leq n$ be maximal so that $|\xi_{k_0}(\omega)| \leq |U|$. Then we first suppose that $k < k_0$. Using the inequality $\log y \leq y - 1$ as in Lemma 6.8, it suffices the estimate the sum

$$S = \sum_{i=1}^{k_0} \frac{|f_a^i(0) - f_b^i(0)|}{|f_b^i(0)|}.$$

Let $\nu_1 < \cdots < \nu_s < n$ be the free return times of ω. Let t be such that $\nu_t \leq k_0 < \nu_{t+1}$. Set $\nu_0 = p_0 = 0$ for convenience. We split up the above sum into the bound orbits and the free orbits: for $j = 0, \ldots, t$, define

$$S_j' = \sum_{i=\nu_j}^{\nu_j+p_j} \frac{|f_a^i(0) - f_b^i(0)|}{|f_b^i(0)|}, \qquad S_j'' = \sum_{i=\nu_j+p_j+1}^{\nu_{j+1}-1} \frac{|f_a^i(0) - f_b^i(0)|}{|f_b^i(0)|}.$$

(We do not sum S_t' further than $i = k_0$, and likewise S_t'' no further than $i = k_0 - 1$.) To estimate S_j'', point (ii) of the previous lemma implies that summing the terms $|f_a^i(0) - f_b^i(0)|$ over $i = \nu_j + p_j + 1, \ldots, \nu_{j+1} - 1$ is bounded by $C \cdot |\xi_{\nu_{j+1}}(\omega)|$. Also,

$|f_b^i(0)| \geq |U|$ for these i by definition of free orbits, so subsequently applying $|\xi_{k_0}(\omega)| \geq |\xi_{\nu_t}(\omega)| \geq 2 \cdot |\xi_{\nu_{t-1}}(\omega)| \geq 4 \cdot |\xi_{\nu_{t-2}}(\omega)| \geq \cdots$, we get

$$\sum_{j=0}^{t} S_j'' \leq C \cdot \frac{|\xi_{k_0}(\omega)|}{|U|} + \sum_{j=0}^{t-1} C \cdot \frac{|\xi_{\nu_{j+1}}(\omega)|}{|U|} \leq C \cdot \frac{|\xi_{k_0}(\omega)|}{|U|} \leq C.$$

For S_j', suppose $\nu_j \leq i \leq \nu_j + p_j$. Since $p_j \ll \nu_j$ by Lemma 6.8, inequality (6.14) holds, to give $|f_b^i(0) - f_a^i(0)| \leq C \cdot |f_a^{i-\nu_j-1}(\xi_{\nu_j+1}(\omega))|$. Together with inequality (6.9), this shows that

$$\begin{aligned} |f_b^i(0) - f_a^i(0)| &\leq C \cdot |Df_a^{i-\nu_j+1}(f_a(0))| \cdot |\xi_{\nu_j+1}(\omega)| \\ &\leq C \cdot |Df_a^{i-\nu_j+1}(f_a(0))| \cdot |f_a(\xi_{\nu_j}(\omega))|. \end{aligned}$$

Similarly, by the definition of the bound orbit,

$$\begin{aligned} |Df_a^{i-\nu_j+1}(f_a(0))| \cdot |f_a^{\nu_j+1}(0) - f_a(0)| &\leq C \cdot |f_a^i(0) - f_a^{i-\nu_j}(0)| \\ &\leq C \cdot e^{-\beta(i-\nu_j)}. \end{aligned}$$

Furthermore, by construction of $\mathscr{E}_{n-1}$, it holds that all $\xi_{\nu_j}(\omega)$ fully contains some I_{r_j,ℓ_j} with $r_j \geq \Delta$, and it holds that $|\xi_{\nu_j}(\omega)| \leq 4 \cdot e^{-r_j}/r_j^2 \leq |U_{r_j}|$. Combining the previous two inequalities, and the fact that f_a has bounded distortion on $\xi_{\nu_j}(\omega)$, we get

$$\begin{aligned} |f_b^i(0) - f_a^i(0)| &\leq C \cdot \frac{|f_a(\xi_{\nu_j}(\omega))| \cdot e^{-\beta(i-\nu_j)}}{|f_a^{\nu_j+1}(0) - f_a(0)|} \\ &\leq C \cdot \frac{|\xi_{\nu_j}(\omega)| \cdot e^{-\beta(i-\nu_j)}}{|U_{r_j}|}. \end{aligned}$$

Now, if $i \leq \nu_j + N$, then $f_a^i(0) \notin W_\delta$. If $i > \nu_j + N$, then since $a \in BA_{n-1}'$ and $i \leq \nu_j + p_j$, we get

$$|f_a^i(0)| \geq |f_a^{i-\nu_j}(0)| - |f_a^{i-\nu_j}(0) - f_a^i(0)| \geq e^{-\alpha(i-\nu_j)} - e^{-\beta(i-\nu_j)} \geq \frac{e^{-\alpha(i-\nu_j)}}{2}.$$

From all this, it follows that

$$S_j' \leq C \cdot \sum_{i=\nu_j}^{\nu_j+p_j} \frac{|\xi_{\nu_j}(\omega)| \cdot e^{-\beta(i-\nu_j)}}{|U_{r_j}| \cdot e^{-\alpha(i-\nu_j)}} \leq C \cdot \frac{|\xi_{\nu_j}(\omega)|}{|U_{r_j}|}.$$

For any positive integer r, define now $(r) = \{j < t : \xi_{\nu_j}(\omega) \cap I_r \neq \varnothing\}$. Since $|\xi_{\nu_{j+1}}| \geq 2 \cdot |\xi_{\nu_{j+1}}|$, we have the estimates

$$\sum_{j=1}^{t} \frac{|\xi_{\nu_j}(\omega)|}{|U_{r_j}|} \leq \sum_{j=1}^{t} \sum_{r=1}^{\infty} \frac{|\xi_{\nu_j}(\omega)|}{|U_r|} \leq C \cdot \sum_{r=1}^{\infty} \max_{j<t} \frac{|\xi_{\nu_j}(\omega)|}{|U_r|} \leq C \cdot \sum_{r=1}^{\infty} \frac{4}{r^2} \leq C.$$

This concludes the case for $k \leq k_0$. For the remaining case we need to estimate

$$\frac{|Df_a^{k-k_0}(f_a^k(0))|}{|Df_b^{k-k_0}(f_b^k(0))|}.$$

It holds that for all $\varepsilon > 0$ and for all Δ, there exists $a_0 < 2$ such that for all $a, b \in [a_0, 2]$, we have

$$\sup_{x \in U_\Delta} |f_a(x) - f_b(x)| < \varepsilon \quad \text{for } j = 1, \ldots, n - k_0.$$

It follows that $d_{\mathrm{H}}(\xi_k(\omega), f_a^{k-k_0}(\xi_{k_0}(\omega))) \leq \varepsilon$ for $k = k_0, \ldots, n-1$. Since $\xi_n(\omega) \subseteq U_{\Delta/2}$, this implies that $f_a^{n-k_0}(\xi_{k_0}(\omega))$ is contained in a small neighbourhood V of 0. By Proposition B.4, there then exists $C > 0$ such that

$$\frac{|Df_2^j(x)|}{|Df_2^j(y)|} \leq C \quad \text{for } j = 0, \ldots, k - k_0.$$

All together, this shows that for all $x, y \in \xi_{k_0}(\omega)$ and $a, b \in \omega$, we have

$$\frac{|Df_a^j(x)|}{|Df_b^j(y)|} \leq C \quad \text{for } j = 0, \ldots, n - k_0.$$

As noted before, a straightforward application of Proposition 6.2 finishes the proof this lemma. ■

Lemma 6.15 is a technical result, and basically its *raison d'être* is to make following sentence rigorous:

> during the free orbit, the interval $\xi_{\nu+p}(\omega)$ is expanded by a factor $e^{\gamma(\nu' - (\nu+p+1))}$, due to Lemma 6.4.

This phrase is a rampant occurrence in the articles by Benedicks & Carleson, but there was some work required to actually show the result. The result also allows us to prove Proposition 6.12 on the exclusion of the parameters satisfying the basic assumption BA.

Proof of Proposition 6.12. If $\omega \in \mathscr{B}_{n-1} | EX_{n-1}$ then there exists a free return $\nu \leq n$ with binding period p such that $\xi_\nu(\omega)$ covers some interval $I_{r,r'}$ with $r \leq \alpha\nu$. Note that $|\xi_n(\omega)| \geq e^{p/4} \cdot |\xi_\nu(\omega)|$ by Lemma 6.16(i), recall that $p \geq C_0 \cdot r$ by Lemma 6.8(iii). It follows that for a_0 close enough to 2, we have

$$|\xi_n(\omega)| \geq e^{p/4} \cdot \frac{e^{-r}}{r^2} \geq \frac{e^{(-1+C_0)r}}{r^2} \geq e^{(-1+C_0)\alpha n}.$$

The same inequality holds if we replace ω by the maximal interval $\tilde{\omega} \subseteq \omega$ such that $\xi_n(\tilde{\omega}) \subseteq U_{\Delta/2}$. Because the distortion of $\xi_n : \tilde{\omega} \longrightarrow I$ is bounded by the Lemma 6.15, it follows that

$$\frac{\left|\bigcup_{r > \alpha n} \omega_{r,\ell}\right|}{|\omega|} \leq \frac{\left|\bigcup_{r > \alpha n} \omega_{r,\ell}\right|}{|\tilde{\omega}|} \leq C \cdot \frac{e^{-\alpha n}}{|\xi_n(\tilde{\omega})|} \leq C \cdot e^{-C_0 \alpha n/2} \leq e^{-C_0 \alpha n/4}.$$

The last inequality follows by taking a_0 sufficiently close to 2. ■

7. Comparing the fold-and-twist map to the Hénon map

Consider the Hénon map for parameters $a \in [0, 2]$, $b > 0$:

$$H_{a,b} : \begin{pmatrix} x \\ y \end{pmatrix} \longmapsto \begin{pmatrix} 1 - ax^2 + y \\ bx \end{pmatrix}.$$

The saddle fixed point given by $x = \frac{1}{2a}(b - 1 + \sqrt{(b-1)^2 + 4a})$, $y = bx$ is of interest. Let W^u denote its unstable manifold. (See any of the books included in the Literature section for a treatment of invariant manifolds; the text by Hirsch, Pugh, & Shub [6] seems to be the standard reference.) Benedicks & Carleson [13] proved the following statement.

Theorem 7.1 (Benedicks and Carleson)**.** *For all $\gamma < \log(2)$ and there exists $b_0 > 0$, such that for all $b \in [0, b_0]$ the following holds. There exists a set $E(b) \subseteq [0, 2]$ of positive Lebesgue measure, such that for all $a \in E$*

(i) *there exists an open set U such that for all $z \in U$*

$$d(H^n(z), \overline{W^u}) \to 0 \qquad \text{as } n \to \infty,$$

(ii) *there exists $z_0 \in W^u$ such $\{H^n(z_0)\}_{n \geq 1}$ is dense in W^u, and*

$$\|DH^n_{z_0}(0, 1)\| \geq e^{\gamma n} \qquad \text{for all } n \geq 1.$$

The results of Theorem 7.1 hold in particular for many small perturbations of b close to 0 and a close to 2. In search for a similar type of perturbation within the parameters of the fold-and-twist map, we consider φ close to 180° and a close to 4. In Figure 20, Lyapunov diagrams are compared of the Hénon map and the fold-and-twist map

$$T_{a,\varphi} : \begin{pmatrix} x \\ y \end{pmatrix} \longmapsto \begin{pmatrix} \cos\varphi & -\sin\varphi \\ \sin\varphi & \cos\varphi \end{pmatrix} \cdot \begin{pmatrix} a(\frac{1}{4} - x^2) - \frac{1}{2} \\ y \end{pmatrix}.$$

For clarity, the colour red now indicates one positive Lyapunov exponent, while the colour black indicates two positive Lyapunov exponents. In both

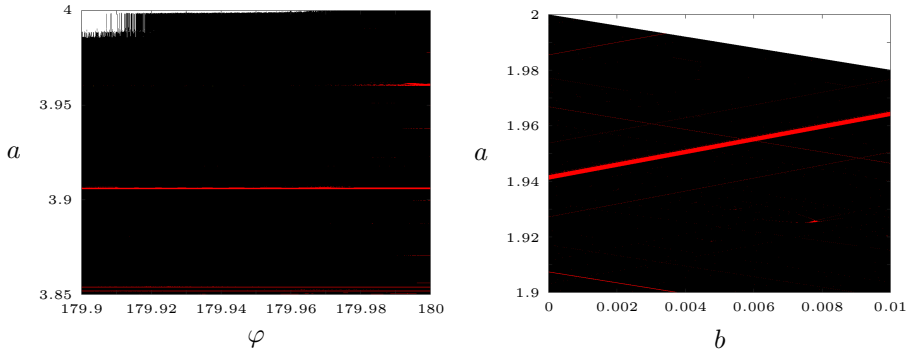

Figure 20: Left: parameter plane of the fold-and-twist map. Right: parameter plane of the Hénon map.

diagrams we observe the following. Fixing a horizontal coordinate seemingly yields a set of red intervals in the vertical direction which, albeit small, have a positive measure in total. Since the sets of positive measure seem to be so similar for both maps, one would think that a similar parameter exclusion procedure could work for the fold-and-twist map as for the quadratic map.

However, reaching a statement as Theorem 7.1 for the fold-and-twist map would be considerably more troublesome. For example, the following necessary basic result for the Hénon map would already be much more work to obtain for the fold-and-twist map.

Lemma 7.2. *For fixed b, there is a segment of W^u going through the fixed point, which is given by the function*

$$\psi(y) = 1 - a\left(\frac{y}{b}\right)^2 + b\sqrt{\frac{1-\frac{y}{b}}{a}} + b^2 r\left(\frac{y}{b}, a\right),$$

where $r \in C^\infty([-\frac{7}{8}, \frac{7}{8}] \times [a_0, 2])$.

One difficulty of the fold-and-twist map is that the chaotic regions do not stem from fixed points, but from higher period points. This brings multiple difficulties along with it, namely

1. one has to work with $T^p_{a,\varphi}$ for some higher p, making exact expressions highly complicated;
2. it is unclear whether exact computation of the periodic points is possible: in Garst & Sterk [18] the only relevant orbits found are of period four;
3. the periodicity p itself is sensitive to parameter regions, creating difficulties in constructing parameter regions of positive measure.

The Hénon map is circumvents all these difficulties by continually possessing a saddle fixed point for which exact expressions are manageable.

Another caveat of Figure 20 is that the presented parameter region is not regular, in the sense that it breaks down very quickly for values $\varphi < 179.9$, as the full diagram in Figure 8 suggests. This does not happen to the diagram of the Hénon map when considering $b > 0.01$. Moreover, computing fold-and-twist orbits corresponding to parameters in the red regions leads to behaviour of the form observed in Figure 12 of the article by Broer et al. [16]. They describe how error accumulation when computing high iterates can lead to large oscillations in dynamical behaviour when normally hyperbolic invariant circles with large slopes. This calls into question the accuracy of the diagram in Figure 20.

Lastly, we have already mentioned that the fold-and-twist map fails to be dissipative, whereas Palis and Takens crucially use this fact to prove that $\mathscr{A} = \overline{W^u}$ for the Hénon map. In detail, their statement is as follows (see Palis & Takens [10], Appendix 3).

Proposition 7.3. *(Palis and Takens) Let $T : \mathbf{R}^2 \longrightarrow \mathbf{R}^2$ be a diffeomorphism with hyperbolic fixed point p, such that*

(i) *there exists a point $q \in W^s(p) \cap W^u(p)$,*

(ii) *$|\det DT(x,y)| < 1$ for all $(x,y) \in \mathbf{R}^2$,*

(iii) *$W^u(p)$ is a bounded set in $\mathbf{R}^2$.*

Then $d(T^n(z), \overline{W^u(p)}) \to 0$ as $n \to \infty$ for all z in some open set $U \subseteq \mathbf{R}^2$.

8. Conclusions and discussion

In pursuit of so called *quasi-periodic Hénon-like* attractors, we have considered the fold-and-twist map $T_{a,\varphi}$ being periodically forced by the Arnold circle map $A_{\alpha,\delta}$, resulting in a novel skew product of the solid torus $\mathbf{R}^2 \times S^1$. We have shed light on the parameter space of the skew product by numerically computing relevant Lyapunov diagrams; such computations had been done before for the Arnold map and fold-and-twist, and are reiterated in this work. This has led to multiple observations concerning the dynamics of the skew product.

Firstly, the Hopf-Neĭmark-Sacker bifurcation observed in the fold-and-twist map appears to be persistent when perturbing the coupling strength in the skew product away from 0. However, the theory of normally hyperbolic invariant manifolds as presented by Hirsch, Pugh, & Shub is inadequate to prove this rigorously. The same problem arises when trying to prove persistence of the invariant circle of $T_{a,\varphi}$ for $\varphi = 90°$. A normally hyperbolic theory for non-smooth manifolds would therefore be desirable.

Secondly, we have found that smooth quasi-periodic normally hyperbolic invariant circles can be found in certain parameter regions of the skew product. Also, by calculating orbits and corresponding Lyapunov exponents, we have provided evidence for chaotic attractors on which the dynamics are 'Hénon-like product quasi-periodic'. However, finding concrete evidence that the unstable manifolds of the saddle invariant circles are indeed related to computed attractors would require more work. Computing the unstable manifolds explicitly, possibly using the methods such as those described by Haro et al. [5], could be direction towards formulating the appropriate conjectures.

On a lower level, proving the existence of quasi-periodic Hénon-like attractors in the skew product probably relies upon the existence of Hénon-like attractors in the fold-and-twist map. The latter question was already raised by Garst & Sterk [18]. Towards finding an answer, an analogy was sought between the fold-and-twist map and the Hénon map, since Benedicks & Carleson [12, 13] famously provided results in the Hénon case. Aided by the detailed text of De Melo & Van Strien [8], the proof for the sensitivity of the quadratic map was restudied and affirmed. However, a direct analogy between the fold-and-twist map, and other non-invertible maps, and the Hénon map remains uncertain. This is mainly due to rapidly fluctuating periodicity of saddle points with respect to the parameter space. It therefore seems more likely to prove said conjures for a set of parameters with positive *one*-dimensional Lebesgue measure — in the case of the fold-and-twist map by fixing a particular angle φ — rather than a whole set of parameters in the plane.

A. Numerical methods

A.1. Lyapunov exponents. We describe the method for calculating the first two Lyapunov exponents of a differentiable map f. (The first two exponents are sufficient for our purposes.) The method is taken from Benettin et al. [15]. Let x_0 be the initial point, and denote by $x_0, x_1, x_2, \ldots$ the orbit of x_0 under f. Fix a time-step s, and start an inductive procedure by taking random orthonormal vectors ξ_0^1, ξ_0^2. At the nth step, set

$$\begin{aligned}
\zeta_n^1 &= Df^s(x_{(n-1)s})\xi_{n-1}^1, & \zeta_n^2 &= Df^s(x_{(n-1)s})\xi_{n-1}^2,\\
\eta_n^1 &= \zeta_n^1, & \eta_n^2 &= \zeta_n^2 - \frac{\langle \zeta_n^2, \zeta_n^1\rangle}{\langle \zeta_n^1, \zeta_n^1\rangle}\zeta_n^1,\\
\ell_n^1 &= \frac{1}{ns}\sum_{j=1}^{n}\log(\|\eta_j^1\|), & \ell_n^2 &= \frac{1}{ns}\sum_{j=1}^{n}\log(\|\eta_j^2\|),\\
\xi_n^1 &= \frac{1}{\|\eta_n^1\|}\eta_n^1, & \xi_n^2 &= \frac{1}{\|\eta_n^2\|}\eta_n^2.
\end{aligned}$$

If $s = 1$, then we are just computing the tangent map of each iterate, and orthogonalising the image vectors. For $s > 1$, the orthogonalisation happens only after every s iterates. The sums $\sum \log(\|\eta_j^i\|)$ are called *Lyapunov sums*, and the numbers ℓ_n^i estimate the ith Lyapunov exponents.

A.2. Rotation numbers. This section describes the method for creating the solid Arnold tongues shown Figure 2. In theory, the Lyapunov exponent of the Arnold map could be used for this: *all* of Arnold tongues are computed at once by the condition that periodic dynamics corresponds to a negative Lyapunov exponent. In practise, this method does clearly present the (p/q)-tongues for small q, but the combination of rasterisation and thinness of the tongues with large q creates a 'white noise' effect which is not reminiscent of the smoothness of the tongues. Instead, a much better result is obtained by only showing the first thousand tongues or so. For this we need to compute the tongues one by one, and thus we need to calculate rotation numbers. The rotation numbers are calculated by simply truncating at $n = 10^5$ the formula

$$\rho = \lim_{n\to\infty}\frac{F^n(0)}{n},$$

where F is a lift of $A_{\alpha,\delta}$. Note that on the interior of the Arnold tongues there exists a stable periodic orbit, to which $F^n(0)$ always converges. (Even if 0 lies precisely on the unstable periodic orbit, computation error will ensure that the computed orbit converges to the stable periodic orbit.) So, in spite of computation error, the formula converges to the true rotation number here. Then, for all fractions p/q with $1 \le q \le 100$, say, we determine whether ρ belongs to the (p/q)-periodic interval of $A_{\alpha,\delta}$ by the criterion

$$\left|\rho - \frac{p}{q}\right| < \varepsilon_0 \cdot \delta^{q-1},$$

where ε_0 is an error constant typically chosen as $\varepsilon_0 = 10^{-6}$. This criterion resembles Arnold's scaling law for the (p/q)-tongue width $\Delta\alpha \le C \cdot \delta^q$.

A.3. Continuation of saddle-node bifurcation. The curves in Figure 4 are computed by continuation of saddle-node bifurcation, which is a technique lying at the heart of the proof of Proposition 3.3. The technique is to fix an initial value of δ and a rational rotation number p/q, and then find a corresponding pair (x, α) by applying Newton's method to the map in (3.1) using the Jacobian in the variables (x, α). Continuation means to shift δ slightly, and reapply Newton's method starting with the solution (x, α) obtained for the previous δ.

B. Some facts about derivatives and distortion

Proposition B.1. *Let $g_a : I \longrightarrow \mathbf{R}$ be any smooth family of maps, and suppose $\sup_{a,x} |\partial_a g_a(x)| \leq C'$. Then we have the inequalities*

$$\begin{aligned} |\partial_a g_a^j(x)| &\leq C' \cdot \sum_{i=0}^{j-1} |Dg_a^{j-1-i}(g_a^i(x))| \\ &\leq C' \cdot |Dg_a^{j-2}(g_a(x))| \cdot \left(|Dg_a(x)| + \sum_{i=0}^{j-2} \frac{1}{|Dg_a^i(g_a(x))|} \right). \end{aligned} \tag{B.1}$$

Proof. The first inequality follows by induction using the formulas

$$\begin{aligned} \partial_a g_a^{j+1}(x) &= \partial_a g_a(g_a^j(x)) + Dg_a(g_a^j(x)) \cdot \partial_a g_a^j(x), \\ Dg_a^{j-i}(g_a^i(x)) &= Dg_a^{j-1-i}(g_a^i(x)) \cdot Dg_a(g_a^j(x)). \end{aligned}$$

The second inequality follows from the formula

$$Dg_a^{j-2}(g_a(x)) = Dg_a^{j-1-i}(g_a^i(x)) \cdot Dg_a^{i-1}(g_a(x)).$$

The verifications are straightforward and therefore omitted. ∎

Recall that $f_2(x) = 1 - 2x^2$ and $T(x) = 1 - 2|x|$. If $\varphi(x) = \sin(\frac{\pi}{2}x)$, then $f_2(x) = (\varphi \circ T \circ \varphi^{-1})(x)$. Note that, for $k = -2^{n-2}, \ldots, 2^{n-2} - 1$, it holds that

$$T^n(x) = \begin{cases} 2^n x - 4k - 1 & \text{if } x \in [\frac{2k}{2^{n-1}}, \frac{2k+1}{2^{n-1}}], \\ -2^n x + 4k + 3 & \text{if } x \in [\frac{2k+1}{2^{n-1}}, \frac{2k+2}{2^{n-1}}]. \end{cases}$$

From this, we have the following proposition.

Proposition B.2. *For almost all $x \in [-1, 1]$, including $x = 1$, it holds that*

$$\lim_{n\to\infty} \frac{1}{n} \log |Df_2^n(x)| = \log(2).$$

Proof. For $x = 1$ it holds that $f_2^n(x) = -1$ for $n \geq 2$, and the result is straightforward. Otherwise, take any point x such that $\varphi^{-1}(x)$ not iterate under T onto any point of the form $k/2^n$. Then by the chain rule

$$Df_2^n(x) = D\varphi((T^n \circ \varphi^{-1})(x)) \cdot DT^n(\varphi^{-1}(x)) \cdot D\varphi^{-1}(x). \tag{B.2}$$

Hence,

$$\log |Df_2^n(x)| = \log |\tfrac{\pi}{2} \cdot \cos(\tfrac{\pi}{2} \cdot (T^n \circ \varphi^{-1})(x))| + \log 2^n + \log |D\varphi^{-1}(x)|.$$

From here the conclusion follows immediately. ∎

Definition B.3. Let $g : V \longrightarrow \mathbf{R}$ be differentiable on some open $V \subseteq \mathbf{R}$, then we define the *distortion* (possibly ∞) of g on a compact interval $J \subseteq V$ as

$$\operatorname{dst}(g, J) = \sup_{x,y\in J} \log \frac{|Dg(x)|}{|Dg(y)|}.$$

The notion of distortion has interesting consequences for g^n when $g^n|_J$ is a diffeomorphism, and the map $x \longmapsto \log|Dg(x)|$ has Lipschitz constant $K < \infty$, that is, g has *bounded* distortion. In particular, we have the following result on the distortion of the Misiurewicz map f_2.

Proposition B.4. *For any neighbourhood $W = (-\delta, \delta)$ of x_0, there exists $C > 0$ such that the following holds. For each interval $[x, y] \subseteq I$ and each $n \geq 1$ such that $f_2^n([x, y]) \subset W$, it holds that*

$$\operatorname{dst}(f_2^n, [x, y]) < C.$$

Proof. The proposition is taken from De Melo & Van Strien [8](see Proposition VI.6.1), but their proof heavily relies on the theory of Misiurewicz maps. Here we give a proof using that f_2 is conjugate to the tent map $T(x) = 1 - 2|x|$. Set $K = \arcsin(\delta) > 0$. Then $f_2^n(x) \in W$ if an only if $|T^n(\frac{2}{\pi}\arcsin(x))| < \frac{2}{\pi}K$, equivalently for some $k = -2^{n-1}, \ldots, 2^{n-1} - 1$,

$$\left|\frac{2}{\pi}\arcsin(x) - \frac{2k+1}{2^n}\right| < \frac{K}{2^{n-1}\pi}, \tag{B.3}$$

or, using $|x - y| \leq |\arcsin(x) - \arcsin(y)|$,

$$\left|x - \sin\left(\frac{\pi(2k+1)}{2^{n+1}}\right)\right| < \frac{K}{2^n}.$$

By equation (B.2), we get

$$\frac{|Df_2^n(x)|}{|Df_2^n(y)|} = \frac{\sqrt{1-y^2}}{\sqrt{1-x^2}} \cdot \frac{|\arcsin(x)|}{|\arcsin(y)|} \cdot \frac{|\cos(\frac{\pi}{2}(T^n(\frac{2}{\pi}\arcsin(x))))|}{|\cos(\frac{\pi}{2}(T^n(\frac{2}{\pi}\arcsin(y))))|}.$$

Using the previous facts, we need to bound each factor on the right hand side. Note that if $f^k[x, y] \subseteq W$, then the integer k in (B.3) has to be the same for both x and y. For the first factor, it follows that for $k = 0, \ldots, 2^{n-1} - 1$,

$$\frac{1-y^2}{1-x^2} \leq \frac{1 - \left(\sin(\frac{\pi(2k+1)}{2^{n+1}}) - \frac{K}{2^n}\right)^2}{1 - \left(\sin(\frac{\pi(2k+1)}{2^{n+1}}) + \frac{K}{2^n}\right)^2}. \tag{B.4}$$

Denote the right hand side of (B.4) by $Q(k, n)$. Fixing k and differentiating $Q(k, n)$ with respect to n, we have

$$\partial_n Q(k,n) = -2K\log(2) \cdot \frac{\pi(2k+1)\cdot a(k,n) + 2^n\big[b(k,n) - \pi(2k+1)\cdot c(k,n)\big]}{d(k,n)^2},$$

where

$$\begin{aligned}
a(k,n) &= (5\cdot 4^n - 4K^2)\cos(\frac{\pi(2k+1)}{2^{n+1}}),\\
b(k,n) &= 4\sin(\frac{\pi(2k+1)}{2^{n+1}})(2K^2 + 4^n\cos(\frac{\pi(2k+1)}{2^n}) + 4^n),\\
c(k,n) &= 2^n\cos(\frac{3\pi(2k+1)}{2^{n+1}}),\\
d(k,n) &= -2K^2 - 2^{n+2}K\sin(\frac{\pi(2k+1)}{2^{n+1}}) + 4^n\cos(\frac{\pi(2k+1)}{2^n}) + 4^n.
\end{aligned}$$

It holds that $\partial_n Q(k,n) \leq 0$ for all $k = 0, \ldots, 2^{n-1} - 1$, because $a(k,n) \geq 2^n \cdot c(k,n)$. This shows that for fixed k, the right hand side of (B.4) decreases as n increases. Therefore, to show that (B.4) is bounded, it suffices to substitute $k = 2^{n-1} - 1$ in the right hand side, and show that the result is bounded for all n. This is indeed the case because taking the limit of the result gives

$$\lim_{n\to\infty} \frac{1 - \left(\sin(\frac{\pi}{2} - \frac{3\pi}{2^{n+1}}) - \frac{K}{2^n}\right)^2}{1 - \left(\sin(\frac{\pi}{2} - \frac{3\pi}{2^{n+1}}) + \frac{K}{2^n}\right)^2} = 1.$$

Bounding the other factors is more straightforward and is hence omitted. ■

Literature

Books on dynamical systems.

[1] M. Brin and G. Stuck, *Introduction to Dynamical Systems*, Cambridge University Press, 2002.

[2] H. W. Broer and F. Takens, *Dynamical Systems and Chaos*, Epsilon Uitgaven, 2009.

[3] P. Collet and J.-P. Eckmann, *Iterated Maps on the Interval as Dynamical Systems*, Birkhäuser, 1980.

[4] R. L. Devaney, *An Introduction to Chaotic Dynamical Systems*, Westview Press, 2003.

[5] A. Haro, M. Canadell, J.-L. Figueras, A. Luque, and J.-M. Mondelo, *The Parameterization Method for Invariant Manifolds: From Rigorous Results to Effective Computations*, Springer, 2016.

[6] M. W. Hirsch, C. C. Pugh, and M. I. Shub, *Invariant Manifolds*, Springer, 1977.

[7] Y. A. Kuznetsov, *Elements of Applied Bifurcation Theory*, 2nd edition, Springer, 1998.

[8] W. C. de Melo and S. J. van Strien, *One-Dimensional Dynamics*, Springer, 1993.

[9] C. Mira, L. Gardini, A. Barugola, and J.-C. Cathala, *Chaotic Dynamics in Two-Dimensional Noninvertible Maps*, World Scientific Publishing, 1996.

[10] J. Palis and F. Takens, *Hyperbolicity and sensitive chaotic dynamics at homoclinic bifurcations*, Cambridge University Press, 1993.

Original articles.

[11] V. I. Arnold, Small denominators. I: Mapping the circle onto itself, *Izvestiya Akademii Nauk SSSR. Seriya Matematicheskaya*, *25*(1), pp. 21–86, 1961.

[12] M. Benedicks and L. Carleson, On iterations of $1 - ax^2$ on $(-1, 1)$, *Annals of Mathematics*, *122*(1), pp. 1–25, 1985.

[13] M. Benedicks and L. Carleson, The dynamics of the Hénon map, *Annals of Mathematics*, *133*(1), pp. 73–169, 1991.

[14] G. Benettin, L. Galgani, A. Giorgilli, and J.-M. Strelcyn, Lyapunov Characteristic Exponents for smooth dynamical systems and for Hamiltonian systems; a method for computing all of them. Part 1: Theory, *Meccanica*, *15*(1), pp. 9–20, 1980.

[15] G. Benettin, L. Galgani, A. Giorgilli, and J.-M. Strelcyn, Lyapunov Characteristic Exponents for smooth dynamical systems and for Hamiltonian systems; a method for computing all of them. Part 1: Numerical application, *Meccanica*, *15*(1), pp. 21–30, 1980.

[16] H. W. Broer, C. Simó, and R. Vitolo, Chaos and quasi-periodicity in diffeomorphisms of the solid torus, *Discrete & Continuous Dynamical Systems - Series B*, *14*(3), pp. 871–905, 2010.

[17] R. E. Ecke, J. D. Farmer, and D. K. Umberger, Scaling of the Arnold Tongues, *Nonlinearity*, *2*(2), pp. 175–196, 1989.

[18] S. Garst and A. E. Sterk, The dynamics of a fold-and-twist map, *Indagationes Mathematicae*, *27*(5), pp. 1279–1304, 2016.

[19] S. Garst and A. E. Sterk, Periodicity and Chaos Amidst Twisting and Folding in Two-Dimensional Maps, *International Journal of Bifurcation and Chaos*, *28*(4), 2018.

[20] M. R. Herman, Sur la conjugaison différentiable des difféomorphismes du cercle à des rotations, *Publications Mathématiques de l'Institut des Hautes Études Scientifiques*, *49*, pp. 5–233, 1979.

[21] L. B. Jonker, The Scaling of Arnol'd Tongues for Differentiable Homeomorphisms of the Circle, *Communications in Mathematical Physics*, *129*(1), pp. 1–25, 1990.

[22] R. S. MacKay and C. Tresser, Transition to topological chaos for circle maps, *Physica D: Nonlinear Phenomena*, *19*(2), pp. 206–237, 1986.

[23] C. Mira, D. Fournier-Prunaret, L. Gardini, H. Kawakami, and J.-C. Cathala, Basin bifurcations of two-dimensional noninvertible maps: Fractalization of basins, *International Journal of Bifurcation and Chaos*, *4*(2), pp. 343–381, 1994.

[24] C. Mira, Noninvertible Maps and Their Embedding into Higher Dimensional Invertible Maps, *Regular and Chaotic Dynamics*, *15*(2–3), pp. 246–260, 2010.

[25] M. Tsujii, A Proof of Benedicks–Carleson–Jacobson Theorem, *Tokyo J. Math*, *16*(2), pp. 295–310, 1993.

Further references.

[26] H. W. Broer, C. Simó, and R. Vitolo, Quasi-periodic Hénon-like attractors in the Lorenz-84 climate model with seasonal forcing, *Equadiff 2003*, pp. 601–606, 2010.

[27] L. Glass, M. R. Guevara, A. Shrier, and R. Perez, Bifurcation and chaos in a periodically stimulated cardiac oscillator, *Physica D: Nonlinear Phenomena*, *7*(1–3), pp. 89–101, 1983.